Journal Pre-proof

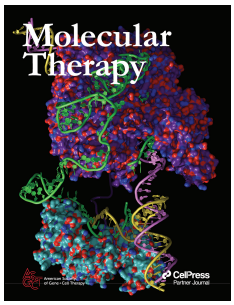

Chimeric Enzymes Enhance Treatment Potential For Globoid Cell Leukodystrophy through Hematopoietic Stem Cell Gene Therapy

Federica Cascino, Alessandra Ricca, Ilaria Picciotti, Erika Valeri, Giulia Unali, Veronica Saporito, Marta Freschi, Francesco Morena, Sabata Martino, Anna Kajaste-Rudnitski, Angela Gritti

PII: S1525-0016(25)00758-0

DOI: https://doi.org/10.1016/j.ymthe.2025.09.030

Reference: YMTHE 7146

To appear in: *Molecular Therapy*

Received Date: 29 August 2025

Accepted Date: 19 September 2025

Please cite this article as: Cascino F, Ricca A, Picciotti I, Valeri E, Unali G, Saporito V, Freschi M, Morena F, Martino S, Kajaste-Rudnitski A, Gritti A, Chimeric Enzymes Enhance Treatment Potential For Globoid Cell Leukodystrophy through Hematopoietic Stem Cell Gene Therapy, *Molecular Therapy* (2025), doi: https://doi.org/10.1016/j.ymthe.2025.09.030.

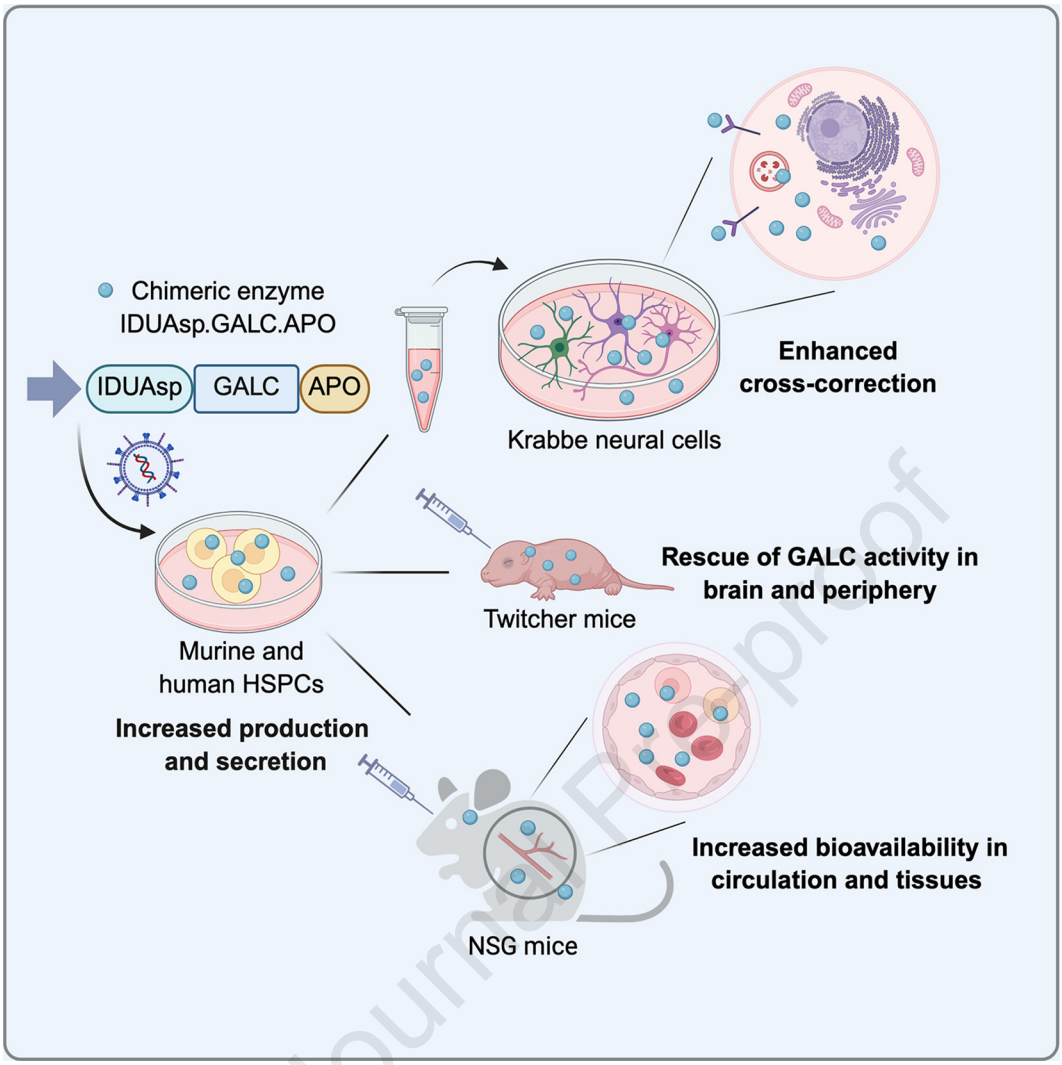

Chimeric Enzymes Enhance Treatment Potential For Globoid Cell Leukodystrophy through Hematopoietic Stem Cell Gene Therapy

Federica Cascino [1*], Alessandra Ricca [1*], Ilaria Picciotti [1], Erika Valeri [1,2], Giulia Unali [1,3], Veronica Saporito [1], Marta Freschi [1,4], Francesco Morena [5], Sabata Martino [5], Anna Kajaste-Rudnitski [1,6], Angela Gritti [1, 7]

1. IRCCS San Raffaele Scientific Institute, San Raffaele Telethon Institute for Gene Therapy (SR-Tiget), 20132 Milan, Italy;
2. Research Institute of Molecular Pathology (IMP), 1030 Vienna, Austria
3. The National Emerging Infectious Diseases Laboratories (NEIDL), University of Boston, Boston, MA 02118, USA;
4. Gene Therapy Program of Dana-Farber/Boston Children's Cancer and Blood Disorder Center, Boston, MA 02215, USA;
5. Department of Chemistry, Biology, and Biotechnology, University of Perugia, 06122 Perugia, Italy;
6. Department of Biology and Biotechnology, University of Pavia, 27100 Pavia, Italy.
7. Vita-Salute San Raffaele University, 20132 Milan, Italy.

*Equal contribution

Corresponding author: Angela Gritti; gritti.angela@hsr.it

ABSTRACT

Globoid cell leukodystrophy (GLD) is a fatal lysosomal storage disorder caused by a deficiency in the β-galactosylceramidase (GALC) enzyme, leading to severe demyelination and neurodegeneration, and often death before the age of two. Hematopoietic stem/progenitor cell transplantation (HSPC-T) has limited efficacy due to inadequate GALC delivery to the central and peripheral nervous systems (CNS, PNS) and associated risks. *In vivo* gene therapy (GT) using adeno-associated viral vectors shows promise, but safety concerns persist. This research presents a strategy using lentiviral vector (LV)-mediated *ex vivo* HSPC-GT with a chimeric GALC enzyme that incorporates peptides from alpha-L-iduronidase (IDUA) and apolipoprotein E II (APO) to enhance expression and blood-brain barrier penetration. The chimeric IDUAsp.GALC.APO enzyme exhibited superior production and secretion compared to native GALC and previous chimeric variants in LV-transduced HSPCs, resulting in improved cross-correction and normalization of GALC activity in GLD neural cells. Proof-of-concept studies demonstrated effective enzyme production, secretion, and cross-correction capability of macrophages from GLD patients. *In vivo* results showed stable gene marking, sustained enzyme production, and efficient delivery of the chimeric GALC in affected organs, including the CNS and PNS. These findings highlight the potential of HSPC-GT using chimeric GALC enzymes as an innovative therapeutic approach for treating GLD.

INTRODUCTION

Globoid cell leukodystrophy (GLD or Krabbe disease) is a severe lysosomal storage disorder (LSD) resulting from a deficiency of β-galactosylceramidase (GALC), an enzyme critical for degrading myelin galactolipids. This enzymatic deficiency leads to the pathological accumulation of substrates such as galactosylceramide (GalCer) and psychosine, triggering neuroinflammation, demyelination, and neurodegeneration in both the central and peripheral nervous systems (CNS, PNS).[1] The early infantile form of GLD is particularly aggressive, often resulting in death before the age of two.[2] The therapeutic options are limited for GLD, with no curative treatments currently available. Correcting protein deficiencies in early-onset LSDs is challenging due to the need for treatments that can quickly and effectively target multiple tissues. A significant obstacle is the blood-brain barrier (BBB), which restricts the delivery of therapeutic proteins to the brain.[3,4,5]

The only approved treatment for GLD is hematopoietic stem/progenitor cell transplantation (HSPC-T) using bone marrow or umbilical cord blood cells. When performed presymptomatically, it can extend lifespan and improve cognitive and motor functions.[6,7,8,9] This approach aims to repopulate the patient's hematopoietic system with donor cells that secrete functional lysosomal enzymes, which surrounding cells can take up through cross-correction.[10] HSPC-T does not entirely prevent CNS and PNS degeneration due to inadequate GALC delivery and limited cross-correction of neurons and glial cells. Despite protocol improvements, HSPC-T still carries significant risks.[11,12] Gene therapy (GT) using adeno-associated viral (AAV) or lentiviral (LV) vectors is being explored as an alternative to enhance GALC expression directly.

In vivo systemic and intracerebral (IC) GT using AAV vectors has shown promise in preclinical GLD models, leading to GALC overexpression, extended survival, and partial correction of pathological hallmarks.[13,14,15] Recent clinical trials evaluate AAV-mediated GT combined with HSPC-T to treat GLD infants (NCT04693598, NCT05739643). The administration of AAVs, primarily through systemic delivery, raises several safety concerns, including hepatic damage,[16,17] dorsal root ganglion toxicity,[14] and genotoxicity.[18,19] These issues arise mainly when a substantial amount of AAV particles reaches peripheral organs due to the high doses required to achieve therapeutic levels in CNS tissues. This situation underscores the necessity for careful long-term monitoring of treated patients[20] and emphasizes the ongoing efforts to enhance vector design and production.[21,22]

Lentiviral (LV)-mediated *ex vivo* HSPC-GT represents a promising alternative to *in vivo* approaches for the treatment of LSDs. This strategy enables sustained, high-level expression of therapeutic proteins from genetically modified autologous HSPCs. Upon reinfusion, these engineered cells successfully engraft within bone marrow niches and differentiate into myeloid lineages, including macrophages and microglia-like cells, mediating long-

lasting therapeutic effects in the PNS and CNS.[23,24] The use of myeloablative conditioning to facilitate HSPC engraftment is a well-established clinical practice, characterized by predictable and manageable toxicity profiles.[25] Furthermore, vector design and promoter optimization advancements have markedly decreased the genotoxicity risks traditionally associated with integrating vectors.[26] Long-term clinical follow-up studies have further confirmed the safety and durability of this approach, demonstrating stable hematopoiesis without malignant transformation in treated patients.[27] The successful application of LV-mediated HSPC-GT in disorders such as metachromatic leukodystrophy (MLD) and mucopolysaccharidosis type I Hurler (MPSIH)[25,28] highlights its therapeutic potential for GLD, despite unique disease-specific challenges remain.

Preclinical studies in Twitcher (TWI) mice, a model mimicking early-onset GLD[29,30], have shown limited benefits of HSPC-GT compared to allogeneic HSPC-T.[31,32,33] Slow brain myeloid cell repopulation and insufficient GALC overexpression in HSPCs and their progeny[31,32] limit the benefits of this approach in rapidly progressing forms that require urgent and widespread enzymatic rescue in the CNS. Additionally, the complex post-translational processing of GALC, essential for proper lysosomal targeting,[34,35] complicates therapy. While other lysosomal enzymes like Arylsulfatase A (ARSA), alpha-L-iduronidase (IDUA), or iduronate 2 sulphatase (IDS) can be safely overexpressed by more than 100 times normal levels in LV-engineered HSPCs,[25,28,36,37,38] GALC typically reaches only 2-3 times normal levels,[39,40] with regulation varying by species, tissue, and cell type.

Enhancing GALC production, secretion, and BBB penetration is critical to maximizing the therapeutic potential of HSPC-GT in GLD. Protein engineering strategies, including signal peptides (sp) for enhanced production and secretion and low-density lipoprotein receptor (LDLr)-binding domains for improved BBB transcytosis, have been shown to boost GT therapeutic benefit in murine models of neurodegenerative LSDs.[37,41,42] *Ex vivo* HSPC-GT using autologous HSPCs engineered for myeloid-specific expression of chimeric IDS fused with Apolipoprotein E II (APO)-derived binding domain is being evaluated in MPSII patients (NCT05665166). Developing chimeric GALC enzymes with enhanced bioavailability is crucial for GLD treatment, though these approaches remain underexplored.[43,44,45]

Our research aims to pioneer HSPC-GT approaches for GLD using chimeric GALC enzymes. In a previous study, we developed LVs with modified murine *Galc* transgenes incorporating the sp from the highly secreted IDS enzyme and the APO domain (IDSsp.m*Galc*.APO). This chimeric enzyme demonstrated superior secretion by LV-transduced neural stem/progenitor cells (NSPCs) and rescued GALC activity in GLD neurons and glia.[40] The advantage of IDSsp.mGALC.APO enzyme was less pronounced in HSPCs, highlighting the transgene- and cell-type-specific protein overexpression and secretion, necessitating further optimization.

To address these challenges, we developed LVs expressing murine and human chimeric GALC enzymes using the IDUAsp to enhance protein secretion. The chimeric enzyme (IDUAsp.GALC.APO) outperformed native GALC and the IDSsp.GALC.APO variant, achieving up to 7-fold and 15-fold the physiological enzymatic activity and improving secretion from LV-transduced murine (Lin^-) and human ($CD34^+$) HSPCs progeny, respectively. This led to superior cross-correction and normalization of GALC activity in patient-derived neural cells. Proof of concept was further shown using GLD patient-derived macrophages, where LV.IDUAsp.h*GALC*.APO restored GALC activity and cross-corrected human GLD-induced pluripotent stem cell (iPSC)-derived neural progeny. *In vivo* studies demonstrated that human HSPCs transduced with LV.IDUAsp.h*GALC*.APO successfully engrafted in immunodeficient mice, leading to enhanced enzyme availability in circulation and delivery to CNS and peripheral tissues compared to the native counterpart. In a severe GLD mouse model, the rapid progression of the disease limited the opportunity to fully demonstrate the therapeutic benefits of the chimeric enzyme within the HSPC-GT approach. Nevertheless, complementary systems, including *in vitro* studies using murine and human cell models and *in vivo* experiments with immunodeficient mice, confirmed the effective production and delivery of the chimeric GALC enzyme across various tissues, including the CNS.

These findings underscore the feasibility and efficacy of LV-mediated HSPC-GT using chimeric GALC enzymes for GLD, highlighting the transformative potential of this approach and warranting further development.

RESULTS

Development and *in vitro* validation of a highly secreted and BBB-targeting murine chimeric GALC enzyme.

Signal peptides (sp) are 5-30 amino acid sequences at the secretory proteins' amino terminus region (N-region). The basicity of the N-polar region and the hydrophobicity of the hydrophobic (H)-core region positively impact protein production and secretion.[46,47,48,49] In a previous study, we developed LVs with a modified *Galc* transgene incorporating the sp from the highly secreted IDS enzyme.[40] The chimeric GALC enzyme demonstrated superior secretion by LV-transduced NSPCs but only a moderate advantage in HSPCs. To enhance GALC biosynthesis and secretion from HSPCs for HSPC-GT applications, we screened sp sequences from various lysosomal enzymes using Peptide 2.0 software (**Table S1**). The IDUAsp showed the highest values of basicity of the N-region (43%) and hydrophobicity of the H-core (93.75%) compared to the sp of other lysosomal enzymes, including GALCsp (0% of basicity and 73,68% of hydrophobicity) and IDSsp (25% of basicity and 64.29% of hydrophobicity). We first generated VSV-G-pseudotyped third-generation LVs encoding a murine (m) GALC enzyme fused to the mCherry fluorescent tag to facilitate protein detection.[40] Then, we engineered the construct by replacing the endogenous GALCsp with the IDUAsp and adding the APO-binding region to enhance BBB crossing[37,42] and improve GALC uptake through LDLr and related proteins expressed in neural cells.[40] The expression of the chimeric mGALC was driven by the ubiquitous human phosphoglycerate kinase (PGK) promoter. We tested the chimeric GALC enzyme (IDUAsp.mGALC.APO) compared to the native mL-mcherry (mGALC) and the previously described IDSsp.mGALC.APO variant (**Figure 1A**)**.** The modifications did not impact LV production, as shown by comparable titers and infectivities of different LV batches (**Table S2**)**.**

We aimed to determine if the IDUAsp provided an advantage over the native GALCsp and the previous IDSsp chimeric variant regarding GALC expression and secretion from HSPCs. We isolated lineage minus (Lin^-) HSPCs from the bone marrow (BM) of 30-35-day-old TWI mice (fully symptomatic) and age-matched wild-type (WT) littermates. We transduced TWI HSPCs with the previously described LVs at 100 multiplicity of infection (MOI). We plated transduced cells and untreated (UT) TWI and WT controls for the colony-forming cell assay (CFC) and myeloid differentiation in liquid culture (LC) to evaluate GALC expression and potential toxicity related to the transduction procedure or transgene overexpression. We observed efficient HSPC transduction (**Figure 1B**) and VCN-dependent supraphysiological GALC activity in the pellet and supernatant (sup) of LV-transduced HSPC progeny (LCs) (**Figure S1A**). The IDUAsp.mGALC.APO exhibited the highest GALC activity, reaching up to 7-fold

(pellet) and 3-fold (sup) the physiological level assessed in UT WT HSPCs (**Figure 1C**). The LV transduction and the consequent GALC overexpression were safe, as demonstrated by a comparable number of colonies originating from UT and LV-transduced TWI HSPCs and UT WT counterparts (CFC assay; **Figure S1B**). Normalizing GALC activity to the VCN highlighted an increased intracellular enzymatic activity of the chimeric enzymes compared to mGALC and the advantage provided by IDUAsp.mGALC.APO compared to IDSsp.mGALC.APO (**Figure 1D).** The increased intracellular GALC activity correlated with the increased enzymatic activity in the sup (**Figure S1C**)**.**

Intracellular GALC processing ensures proper lysosomal targeting and function. The GALC precursor protein (80 kDa) undergoes glycosylation and is trafficked to the lysosomes. In the acidic lysosomal environment, it is proteolytically cleaved into a 50 kDa N-terminal and a 30 kDa carboxyl-terminal subunit, which combine to form a functional enzyme complex.[34,50] Qualitative confocal immunofluorescence (IF) and quantitative ImageStream analyses in LV-transduced HSPC progeny (LC) confirmed the lysosomal localization (LAMP1) of the chimeric IDUAsp.mGALC.APO enzyme (**Figure S1D-E;** proximity index = 88%), as previously described for mGALC and IDSsp.mGALC.APO counterparts.[40]

A fraction of the GALC precursor protein escapes the sorting pathway and is secreted in the extracellular space for uptake by surrounding cells in the cross-correction mechanism.[51] Western blot (WB) analysis using an anti-mCherry antibody confirmed the presence of the GALC precursor protein (molecular weight ~110 kDa, consisting of the 80 kDa GALC precursor fused to the 30 kDa mCherry tag) in the sup of LV-transduced HSPC progeny (**Figure 1E**). These findings suggest that, similarly to mGALC and IDSsp.mGALC.APO, the IDUAsp.mGALC.APO fusion protein is efficiently secreted, making it available for cross-correction of neighbouring cells. Furthermore, WB analysis with an anti-GALC antibody detected both the precursor and cleaved forms of GALC in the LV-transduced HSPC progeny cell pellets, providing evidence for proper expression and intracellular processing of the enzyme (**Figure 1E**). To quantitatively evaluate enzyme production and secreted enzyme specifically available for cross-correction, we performed an ELISA assay detecting mCherry (a surrogate marker for GALC) in pellets and sup of LV-transduced HSPC progeny (LC), respectively. The analysis revealed a significant increase in the expression of the chimeric construct containing IDUAsp compared to the mGALC and IDSsp counterparts (**Figure 1F**)**.**

The APO tag did not affect the half-life of the chimeric proteins, as shown by the similar concentration of mCherry detected over 24 hours in the sup of LV.m*Galc* and IDUAsp.m*Galc*.APO-transduced cells (**Figure 1G**).

The APO domain provided a significant advantage in the transcytosis of GALC in a simplified *in vitro* BBB model using bEND.3 endothelial cells in a transwell system (**Figure 1H**). This result confirms the potential for

enhanced BBB penetration of APO-tagged lysosomal enzymes.[37,52] Additionally, WB analysis with an anti-mCherry antibody revealed the presence of the GALC precursor protein fused to the mCherry tag (110 kDa) in the sup collected from the lower chamber of the transwell. In contrast, the mCherry tag alone (30 kDa) was undetectable (**Figure 1I**). The data confirmed the accuracy of the ELISA assay in detecting GALC precursor form, the variant potentially available for cross-correction.

The findings demonstrate that the chimeric IDUAsp.mGALC.APO enzyme exhibits superior intracellular expression and secretion compared to mGALC and IDSsp.mGALC.APO counterparts, with the APO domain enhancing transcytosis by endothelial cells without altering the enzyme's half-life, highlighting the potential for increased enzyme bioavailability in HSPC-GT settings.

Chimeric GALC enzymes secreted by HSPC progeny rescue GALC activity and reduce intracellular GalCer storage in TWI neural cells.

To optimize *ex vivo* HSPC-GT, chimeric GALC enzyme released by GALC-overexpressing HSPC progeny should be internalized and transported to lysosomes of GALC-deficient neurons and glial cells. To compare the cross-correction capacity of the native and chimeric GALC enzymes, we cultured UT WT, LV.m*Galc*-, LV.IDSsp.m*Galc*.APO-, and LV.IDUAsp.m*Galc*.APO-transduced TWI HSPCs for 14 days (LC; donor cells, **Figure 1B**). The sup of donor cells collected every 24 hours for the last 3 days of culture was used to treat UT, TWI, and NSPC-derived neural progeny (acceptor cells; 72 hours of treatment) (**Figure 2A**). At the end of the experiment, we assessed GALC enzymatic activity, protein uptake, and GalCer storage in cross-corrected (XC) acceptor cells.

The sup collected from UT WT donors partially restored GALC activity in XC TWI neural cells, achieving ~27% of the physiological levels (measured in WT neural cells). The sup from LV.m*Galc*- and LV.IDSsp.m*Galc*.APO-transduced donors significantly enhanced intracellular GALC activity in acceptor TWI cells, reaching ~40-50% of physiological levels. However, only the sup from LV.IDUAsp.m*Galc*.APO-transduced donors normalized GALC activity in acceptor TWI cells (**Figure 2B**). The increased GALC activity in the donor cell sup correlates with intracellular enzymatic activity observed in the cross-corrected cells (**Figure S1F**)**.** Importantly, using equal GALC precursor input, we detected higher concentrations of mCherry in acceptor cells exposed to the sup enriched with IDUAsp.mGALC.APO protein (**Figure 2C**). This finding suggests a more efficient uptake by TWI neural cells, likely mediated by the expression of LDLr and related pathways.[40]

Confocal IF analysis demonstrated comparable clearance of GalCer storage in all XC cells (**Figure 2D**), indicating that ~20% of the physiological intracellular enzymatic activity is sufficient to mediate substrate degradation under the *in vitro* culture conditions tested.[40]

These findings highlight the superiority of the chimeric IDUAsp.mGALC.APO in promoting GALC uptake and restoring enzymatic activity in cross-corrected TWI neural cells, underscoring its potential to enhance the efficacy of HSPC-GT for GLD, warrants further investigation in human-relevant *in vitro* models.

Exploiting chimeric GALC enzymes for *ex vivo* HSPC-GT in TWI mice.

We evaluated the safety and efficacy of HSPC-GT using chimeric GALC enzymes in TWI mice, a GLD model resembling the severity of the infantile GLD forms. Considering the early post-natal psychosine storage in TWI nervous tissues,[53,54] we envisaged performing HSPC transplantation at postnatal days (PND) 2-3 following Busulfan (BUS) conditioning. BUS was selected over total body irradiation (TBI) since it reduced tissue inflammation (**Figure S2A**), improved GALC activity restoration (**Figure S2B**), and enhanced survival (**Figure S2C**) with a lower engraftment rate (**Figure S2D**)**.**

We transplanted neonatal TWI mice with TWI Lin$^-$ HSPCs transduced with LVs encoding m*Galc* constructs (**Figure 3A**)**.** As control, transplantation using WT Lin$^-$ HSPCs transduced with the LV.GFP (green fluorescent protein) was employed (VCN ~6 in LC). The GALC activity of LC cultures from LV.GFP-transduced cells (~24 nmol/h × mg) were comparable to UT LC counterparts (~22 nmol/h × mg). The GALC activity of LV-transduced Lin$^-$ TWI HSPC~~s~~ progeny is shown in **Figure 1B**. The average engraftment in the PB of BUS-conditioned transplanted mice was ~15%, regardless of the treatment (**Figure 3B**), lower than reported for PND 7–9 TWI mice receiving tBM from WT donors after TBI conditioning.[54] We applied the BUS protocol for tBM transplantation in PND 2–3 TWI mice to exclude potential technical issues, achieving ~50% engraftment (**Figure S3A**). We observed modest engraftment of HSPC-derived myeloid cells in the CNS of HSPC-transplanted mice (**Figure S3B**). This correlates with the reduced survival of HSPC-transplanted mice compared to tBM-T counterparts (**Figure S3C**), highlighting the difficulties in achieving effective HSPC engraftment in this model.

TWI mice with HSPC-GT treatment showed lower body weight than WT mice (**Figure 3C**). They experienced a modest increase in average lifespan (42 days) compared to TWI controls (39 days) (**Figure 3D**). The GALC activity was restored to normal or even supranormal levels in the BM, liver, and spleen, the first organs reached

by transplanted HSPCs. We observed a substantial restoration of GALC activity in the transplanted mice's PNS and CNS, achieving up to 70% and 40% of WT levels, respectively (**Figure 3E**)**.**

IF analysis showed that LV-transduced HSPC-derived progeny engrafted throughout the brain parenchyma of recipient TWI mice (**Figure 4A;** GFP$^+$ and mCherry$^+$ cells). The chimeric enzyme was correctly produced and secreted by LV-transduced CD68$^+$ myeloid progeny and was efficiently recaptured by GFAP$^+$ astrocytes (**Figure 4B-B'**) and NeuN$^+$ neurons (**Figure 4C-C'**), where it localized in lysosomes (LAMP1$^+$, **Figure 4D-D'**). These findings suggested that donor-derived myeloid progeny effectively cross-corrected GALC-deficient neuronal and glial cells. To establish proof of concept (PoC) for *in vivo* cross-correction, we employed TWI mice that had undergone tBM-T, a model previously shown to display more consistent donor cell engraftment. This approach was chosen to overcome the limitation observed in HSPC–GT–treated mice, in which the low brain chimerism resulted in insufficient yields of engrafted CD45$^+$ cells for reliable isolation and downstream analysis. In brain tissues from tBM-T TWI mice, we detected GALC enzymatic activity in CD45$^-$ cells—presumed endogenous deficient brain cells—at approximately 30% of WT levels, indicative of effective cross-correction (**Figure S3D**). These findings suggest that HSPC-GT effectively delivers functional GALC enzymes to the affected areas despite modest donor chimerism in hematopoietic and brain tissues. This results in a substantial, even if partial, restoration of GALC activity in the CNS and PNS, key therapeutic targets in GLD, and complete enzymatic correction in peripheral organs.

LVs expressing chimeric hGALC enzymes mediate effective and safe gene transfer in human CD34$^+$ HSPCs and CD14$^+$ monocytes.

We evaluated the efficacy and safety of chimeric human (h) GALC enzymes in clinically relevant human hematopoietic cells. We used a VSV-G-pseudotyped third-generation LV backbone previously used in the HSPC-GT clinical trial for MPSI.[25] We engineered a codon-optimized h*GALC* sequence[32] (LV.h*GALC*) by replacing the GALCsp with the IDSsp and IDUAsp, and included the APO sequence to generate LV.IDSsp.h*GALC*.APO and LV.IDUAsp.h*GALC*.APO (**Figure 5A**). These modifications are intended to enhance enzyme production, secretion, and targeting efficiency, similar to the murine version.

Pilot transductions in BM-derived CD34$^+$ HSPCs from healthy donors (HDs) using LV.GFP and LV.IDSsp.hGALC.APO (50 and 100 MOI) with cyclosporine H (CsH) as a transduction enhancer,[55] determined the optimal culture conditions for maximizing VCN and GALC overexpression without cytotoxic effects. CsH improved

transduction efficiency compared to the vehicle (DMSO), at 5 days post-transduction (**Figure S4A**)**.** This resulted in increased VCN and GALC activity in HSPC-derived progeny (LC) at 14 days post-transduction (**Figure S4B-C**), with no observed toxicity related to LV transduction, CsH, or GALC overexpression (**Figure S4D**).

Based on these results, we selected a dose of 100 MOI to transduce HD CD34$^+$ HSPCs from mobilized (m) PB with LV.h*GALC*, LV.IDSsp.h*GALC*.APO, and LV.IDUAsp.h*GALC*.APO (**Figure 5A**) in the presence of CsH. The transduction was efficient, resulting in a VCN-dependent GALC activity (**Figure 5B, Figure S5A**) and an increase in mRNA expression of the exogenous h*GALC* transgene while the levels of the endogenous h*GALC* remained stable (**Figure S5B**). The transduction procedure and transgene expression did not adversely affect cell growth, colony formation (**Figure S5C-D**)**,** or the composition of LC and CFC populations (**Figure S5E-F**) when comparing LV-transduced cells to UT CD34$^+$ HSPC progeny. Furthermore, the LV transduction led to significantly elevated levels of GALC activity compared to physiological levels found in UT cells, with the IDUAsp.hGALC.APO variant exhibiting a remarkable 15-fold increase over normal levels (**Figure 5C**). Notably, IDUAsp.hGALC.APO outperformed hGALC and showed a 1.3-fold increase in GALC activity normalized for VCN compared to IDSsp.hGALC.APO (**Figure 5C**). Consequently, we selected LV.IDUAsp.h*GALC*.APO for further characterization.

WB analysis confirmed the correct production and secretion of the IDUAsp.hGALC.APO precursor protein (80 kDa) and the presence of the cleaved forms (50 kDa and 30 kDa) (**Figure 5D**). The IDUAsp.hGALC.APO was produced and secreted more than the hGALC protein (**Figure 5E**). Confocal IF analysis on HSPC-derived progeny confirmed the presence of the IDUAsp.hGALC.APO enzyme in lysosomes (**Figure S5G-H**). We evaluated the effectiveness of LV.IDUAsp.h*GALC*.APO in restoring GALC enzymatic activity in patient-derived macrophages, a relevant model for assessing the therapeutic potential of the chimeric GALC enzyme in the context of HSPC-GT. We successfully transduced CD14$^+$ monocytes isolated from the PB of two late-infantile GLD patients and six HDs using either LV.h*GALC* or LV.IDUAsp.h*GALC*.APO (**Figure 5F**). The transduced monocytes were differentiated into macrophages following an established protocol.[56] After 9 days in culture, LV-transduced HD macrophages showed GALC overexpression at ~11-fold the physiological levels. Notably, HD macrophages were transduced with LV.IDUAsp.h*GALC*.APO showed a 2-fold increase in extracellular GALC activity compared to those transduced with LV.h*GALC*. In macrophages derived from GLD patients, GALC activity was restored to physiological or supraphysiological levels following LV transduction (**Figure 5G**).

These *in vitro* findings demonstrated the safety and enhanced intra- and extracellular GALC activity of the chimeric IDUAsp.hGALC.APO enzyme by LV-transduced HSPC progeny, establishing it as a promising candidate for the HSPC-GT approach in treating GLD.

Chimeric hGALC enzymes secreted by human CD14$^+$ and CD34$^+$ HSPC progeny cross-correct GLD-derived neural cells.

We evaluated the cross-correction potential of native hGALC and chimeric IDUAsp.hGALC.APO, produced by engineered CD14$^+$-derived macrophages and CD34$^+$ HSPC progeny (donor cells, shown in **Figure 5C and 5G**) in GALC-deficient neuronal/glial mixed cultures from patient-induced pluripotent stem cells[57] (iPSCs), exposed for 24 hours to sup collected from LV-transduced donor cells.

The sup from LV-transduced GLD macrophages partially restored GALC activity in acceptor cells (XC), achieving up to normal values observed in HD hiPSC-derived neural cells (**Figure 5H**). Notably, the sup from LV.h*GALC*-transduced CD34$^+$ HSPC progeny restored GALC activity to 70% of HD values in GLD neural cells. GALC activity reached physiological levels in cells treated with IDUAsp.hGALC.APO-enriched sup (**Figure 5I**). A functional GALC enzyme is necessary for degrading psychosine, a toxic lipid accumulating in the brain tissues of GLD patients and GLD hiPSC-derived neural cells.[57] The cross-correction mediated by IDUAsp.hGALC.APO was associated with a significant reduction in psychosine levels within 24 hours of treatment in GLD XC neural cells (**Figure 5J**).

These findings demonstrate that both the hGALC and chimeric IDUAsp.hGALC.APO enzymes, secreted by transduced human HSPC progeny and macrophages, restore GALC activity in GLD human neural cells *in vitro*. The chimeric IDUAsp.hGALC.APO enzyme showed superior efficacy in reducing psychosine accumulation in this disease-relevant CNS model, underscoring its potential to enhance the therapeutic efficiency of HSPC-based gene therapy for GLD.

LV.IDUAsp.h*GALC*.APO-transduced CD34$^+$ HSPCs engraft in immunodeficient NOD scid gamma mice and release the chimeric GALC enzyme.

To assess the safety of *in vivo* production and secretion of chimeric hGALC enzymes in HSPC-GT, we transplanted mPB-derived HD CD34$^+$ cells transduced with LV.IDUAsp.h*GALC*.APO, LV.h*GALC*, or LV.GFP (used as control; VCN ~3) into irradiated female immunodeficient NOD scid gamma (NSG) mice. We monitored the

presence of genetically corrected circulating human cells by performing flow cytometry analysis on PB samples collected monthly from the treated mice, starting four weeks after transplantation. The results showed a gradual increase in human hematopoietic cell engraftment ($hCD45^+$) peaking at 8 weeks with a 20% chimerism. Cell engraftment moderately decreased by 12 weeks with no significant differences observed among the treatment groups at any time (**Figure 6A**).

We observed increased GALC enzymatic activity in the serum of mice transplanted with LV.IDUAsp.h*GALC*.APO- and LV.h*GALC*-transduced cells compared to those transplanted with LV.GFP-transduced cells (controls) at 8 weeks (**Figure 6B**). Normalizing the serum enzymatic activity to the PB engraftment highlighted superior secretion and enhanced enzyme bioavailability in the bloodstream of mice receiving LV.IDUAsp.h*GALC*.APO- compared to those receiving LV.h*GALC*-transduced cells (**Figure 6C**).

At the time of sacrifice (16 weeks), the VCN in the BM of treated mice confirmed persistent engraftment and gene marking (**Figure 6D**). We detected comparable levels of $hCD45^+$ and $hCD34^+$ cells in the BM across the different groups (**Figure 6E**). Additionally, the composition of the cell populations was similar, including $hCD34^+hCD38^{+/-}$ (progenitors), $hCD33^+$ (myeloid cell), and $hCD19^+$ (B lymphocyte) populations (**Figure 6F**). In NSG mice transplanted with LV.IDUAsp.h*GALC*.APO- and LV.h*GALC*-transduced cells, we evaluated GALC activity in the spleen and liver, representing the early colonization targets of transplanted cells, and in CNS and PNS tissues, critical therapeutic targets in the disease. We observed a marked increase in GALC activity in the spleen of GT-treated mice (**Figure 6G**). By normalizing the enzymatic activity to the percentage of spleen engraftment (% of $CD45^+$ cells), we highlighted a superior contribution of IDUAsp.hGALC.APO to GALC activity in this organ (**Figure 6G**). We observed a similar advantage when we normalized GALC activity to the percentage of PB engraftment at 12 weeks, both in the spleen (**Figure 6H**) and the liver (**Figure 6I**). These results suggest that the chimeric enzyme reaches the target tissues more efficiently than the unmodified counterpart, enhancing GALC bioavailability. The engraftment of donor cells in the CNS is minimal in this experimental setting due to the sublethal conditioning regimen (A.R., data not shown). By normalizing GALC activity in the CNS tissues of transplanted mice to the percentage of PB engraftment at 12 weeks, we highlighted the advantage of the IDUAsp.hGALC.APO compared to the native counterpart (**Figure 6J**). This result suggests that the circulating chimeric enzyme can cross the BBB.

The chimeric enzyme is more available in the serum, spleen, and liver tissues than the native GALC. The indirect evidence suggesting the ability to cross the BBB further emphasizes its superior biodistribution *in vivo*. These promising results support further investigation in advanced pre-clinical settings.

DISCUSSION

We have engineered chimeric murine and human GALC enzymes with enhanced production, secretion, BBB penetration, and cross-correction capacity. Our modifications enhance enzyme performance in murine and human *in vitro* disease models and *in vivo* HSPC-GT settings.

Previous studies have explored chimeric GALC enzymes with modifications like sp changes and apolipoprotein-derived binding domains. While these studies, mostly in human cell lines or fibroblasts, showed mixed results *in vivo*, the safety and efficacy in HSPC-GT settings remain underexplored.[43,44,45] Our earlier work found that replacing GALCsp with IDSsp increased GALC production and secretion in neural progenitors derived from TWI mice,[40] suggesting this strategy has therapeutic potential. However, the benefits were less pronounced in HSPCs, the key cells in HSPC-GT, highlighting cell-specific differences in GALC production and secretion[39,58,59] and supporting the need for further optimization in these cells. We focused on the IDUAsp for its favourable biophysical properties, which are expected to enhance GALC synthesis and secretion.[46,47,48,49]

In HSPC-GT, reliance on enzyme transport across the BBB is reduced since the engrafted myeloid cells are the primary source of functional enzyme. However, previous studies in MPSII mice showed that HSPCs engineered to express the chimeric IDS enzyme (IDS.ApoEII) achieved better CNS pathology rescue compared to unmodified IDS[37,42] due to increased enzymatic activity and improved transcytosis across brain endothelial cells, supporting clinical translation (NCT05665166). Our study confirms that while the APO modification did not impact GALC production and secretion in neural and hematopoietic cells,[40] it did enhance the transendothelial transfer of the chimeric enzyme in a brain endothelial cell model. The IDUAsp.mGALC.APO enzyme provided superior cross-correction of TWI neurons and glia compared to native and IDSsp-modified GALC enzymes, indicating its potential to cross the BBB and boost GALC supply in the brain. Additionally, APO may enhance GALC uptake in neural cells via LDL receptors[40] as shown for other lysosomal enzymes,[37,41,52] potentially improving therapeutic outcomes.

The IDUAsp.mGALC.APO variant achieved significantly higher GALC enzyme production, reaching a 7-fold increase over the physiological level, compared to the 1.5 - 3-fold increase seen with similar transduction efficacy in previous studies.[31,39,40] This variant also outperformed both native mGALC and the IDSsp.mGALC.APO in terms of expression and release, as indicated by mCherry concentration in the sup-and pellets, and higher enzymatic activity after correcting for VCN. While this level of GALC activity in donor cells is not as extreme as the 50 -100-fold increase observed with other lysosomal enzymes like ARSA or IDUA,[23,36,38] it still holds promise for treating

GALC deficiency if combined with robust donor chimerism and effective enzyme delivery. The GALC precursor protein was efficiently secreted by HSPCs and myeloid progeny and taken up by TWI neurons and glia, providing complete rescue of GALC activity (compared to partial rescue mediated by the native mGALC and the IDSsp.mGALC.APO variant). Excessive GalCer storage in TWI neural cultures can be effectively reduced with minimal GALC levels, such as those in the sup of WT cells.[40] This limitation of the *in vitro* model restricts our ability to detect differences among constructs regarding their cross-correction capacity through residual substrate detection. The complete clearance of GalCer in TWI neuronal and glial cell cultures suggests that the chimeric enzyme operates within the lysosomes of the acceptor cells. Furthermore, the restoration of enzymatic activity and the increased GALC-mCherry content in cross-corrected cells, with equal amounts of GALC-mCherry precursor in the sup, strongly support the effectiveness of the IDUAsp.m*Galc*.APO construct. This highlights the potential of IDUAsp.mGALC.APO to mediate sustained myeloid-mediated cross-correction, thereby contributing to therapeutic benefits in HSPC-GT, in addition to the known neuroprotective and immunomodulatory effects.[60]

Psychosine accumulation and neuroinflammation begin in neonatal TWI mice[53,54] and worsen over time, leading to symptom deterioration and death by postnatal days 35-40, with an average lifespan of 39 days in our Twitcher colony. To improve therapeutic outcomes, we performed HSPC transplantation at PND2, earlier than in previous studies that used PND7.[31,54] Additionally, we used BUS as a myeloablative agent known to enhance donor brain cell engraftment in pre-clinical models[24] as well as in clinical HSPC-GT for LSDs.[25,61] While the timing of CNS engraftment after TBI and BUS has been extensively investigated in adult settings,[24,62,63,64] fewer studies explore early postnatal (PND7-10) transplantation in GLD models using TBI[31,32,54] or BUS.[65,66,67] We adapted a neonatal BUS conditioning protocol[68] and found that BUS-conditioned mice showed improved survival and GALC activity rescue compared to TBI-conditioned mice. Hematopoietic cell engraftment was similar in WT and TWI mice. However, the engraftment of Lin^- cell was lower than that of WT tBM cells, which aligns with prior findings indicating that committed progenitors engraft faster than stem cells.[69,70] Although HSPC engraftment in TWI mice was lower than reported in previous studies,[31,32] increasing BUS dose or irradiation was not feasible due to high neonatal mortality. Other compounds that can enhance brain engraftment have been identified, such as Pexidartinib (PLX), a small molecule that inhibits the colony-stimulating factor 1 receptor.[63,71,72,73] However, there is a lack of data regarding the feasibility, optimal dosage, and effects of PLX use in neonatal mice. Despite the low engraftment, BUS-conditioned TWI mice showed significant levels of GALC reconstitution, reaching close to normal levels in peripheral organs and PNS, and approximately 30-40% of normal levels in CNS tissues. These levels are comparable to those reported in prior studies using tBM-T or HSPC-GT, in which GALC reconstitution

was achieved with significantly higher donor chimerism (80–90%).[31,32,54] These findings highlight the efficacy of the HSPC-GT approach using a chimeric GALC enzyme, which can achieve therapeutically relevant levels of enzyme activity even in the context of limited engraftment.

Our study demonstrates that the chimeric GALC secreted by donor-derived HSPC progeny can effectively cross-correct GALC-deficient CNS cells *in vitro,* both in murine and human contexts. Moreover, we provide qualitative *in vivo* evidence of donor-derived transgenic GALC protein in TWI mice's neurons and glial cells following HSPC-GT. Quantitative assessment of cross-correction within the CNS *in vivo* remains technically challenging, particularly in the context of low donor cell chimerism in brain tissues. To address this limitation, we employed an allogeneic transplant model in TWI mice using tBM to achieve high donor chimerism in both PB and CNS compartments. In this setting, we observed that GALC enzymatic activity was restored to approximately 30% of normal levels in freshly isolated $CD45^{-}$ brain cells (putative endogenous brain cells), providing strong evidence that myeloid-to-neural cross-correction occurs *in vivo* and may contribute to enzyme reconstitution in recipient GALC-deficient brain cells. These findings offer a critical perspective, especially in light of previous reports suggesting limited or negligible cross-correction *in vivo* in GLD models.[74] While differences in experimental models, transgene constructs, or assessment techniques may explain some discrepancies across studies, our results support the notion that cross-correction is a relevant mechanism contributing to the therapeutic benefit of HSPC-T and HSPC-GT in lysosomal storage disorders. Further studies will be essential to validate these findings, optimize cross-correction efficiency in the HSPC-GT setting, and elucidate the cellular and molecular pathways involved in GALC uptake, trafficking, and activity within different CNS cell populations.

The limited therapeutic improvements in TWI mice undergoing HSPC-GT highlight key study constraints. Effective restoration of GALC activity, a sensitive marker for assessing therapeutic benefits, relies on proper engraftment of donor HSPCs. The TWI model’s aggressive neurological progression necessitates neonatal intervention, yet the BUS conditioning protocol poses toxicity risks, leading to inadequate myeloablation and modest engraftment. This, along with the slow microglial and macrophage replacement in the CNS following HSPC-GT, limits enzymatic rescue and the neuroprotective functions of donor cells. When combined with accelerated disease progression, these factors likely explain the limited therapeutic benefits and the lack of advantage of the chimeric enzyme over native GALC. Importantly, these challenges are specific to the TWI model and do not apply to neonatal GLD patients.[6,7] Thus, while these murine model limitations are acknowledged, they do not undermine the potential of the chimeric construct, warranting further investigation. Future studies in GLD

murine models with slower disease progression[75] will evaluate the efficacy of the chimeric GALC enzyme in enhancing treatment benefit in HSPC-GT and, potentially, in *in vivo* GT approaches targeting the CNS.

Despite similarities between human and murine GALC enzymes, protein folding, stability, and catalytic efficiency differences may influence their functional performance *in vivo*.[35] Our study observed reduced expression levels of human GALC compared to murine GALC when expressed in murine HSPCs (**Figure S5I**)**.** This discrepancy may be attributed to species-specific factors such as mRNA stability or differences in post-translational processing.[59] These data highlight the importance of performing human-specific studies to accurately evaluate the therapeutic potential and expression profile of human GALC, particularly in translational and preclinical settings. By utilizing an optimized LV backbone[25] and *GALC* codon optimization,[32] we developed an LV.IDUAsp.h*GALC*.APO analogous to the murine version. When coupled with CsH as a transduction enhancer,[55] we achieved a 15-fold increase over normal GALC activity in human HD-derived HSPCs. This increase exceeds the maximum 3-fold enhancement reported previously.[32] The chimeric hGALC enzyme demonstrated superior expression and activity compared to the native hGALC and the IDSsp.hGALC.APO variant in human HSPCs. Additionally, it was more effective in reducing psychosine storage in GLD human neurons and glial cells. The successful production and secretion of IDUAsp.hGALC.APO by patient-derived macrophages and its effective cross-correction of GLD neurons and glial cells confirms its potential for therapeutic application in a pathological context. Considering the inherent high variability when using primary cells, data from only two patients limit our ability to establish the superiority of the chimeric construct in this specific setting. Still, the rarity of these samples restricted our capacity to perform more replicates. Despite these challenges, we confirmed that both vectors could effectively transduce GLD samples, providing proof of concept for the functionality of the *GALC* constructs in these cell types and confirming the cross-correction ability of the secreted chimeric GALC.

Our xenotransplantation studies using NSG mice - an established model for assessing the efficacy of HSPC-GT and long-term gene marking in the human context - demonstrated the efficient engraftment of transduced HSPCs. In this system, HSPCs engineered to express the chimeric GALC enzyme led to increased GALC activity in serum and spleen compared to control groups, despite similar or lower engraftment levels. As expected, donor cell engraftment in other tissues, such as the liver and brain, was limited, reflecting a well-recognized limitation of the NSG xenotransplant model.[76] This constraint made detecting significant increases in GALC enzymatic activity in these organs challenging. However, when GALC activity was normalized to the percentage of donor cells in PB, a relative enrichment was observed in the spleen, liver, and brain, suggesting that the chimeric GALC enzyme exhibits improved bioavailability and tissue penetration. This finding suggests improved enzyme systemic

458 bioavailability could reduce vector dosage and enhance the therapy's safety. Overall, these *in vitro* and *in vivo*
459 results underscore the importance of myeloid-mediated cross-correction in CNS cells as a key mechanism
460 contributing to the therapeutic efficacy of HSPC-GT in LSDs. Additionally, they suggest that the APO modification
461 enhances GALC delivery to the brain and reduces storage, similar to previous findings reported for IDS[37] and
462 ARSA enzymes.[52]

463 In summary, our findings underscore the potential of the IDUAsp.GALC.APO variant, combined with optimized
464 HSPC transplantation methods, to significantly enhance therapeutic outcomes of HSPC-GT for GLD. This
465 construct enables robust enzyme production, efficient secretion, and widespread tissue bioavailability, ultimately
466 facilitating enzymatic correction across all affected organs and systems.
467

Materials and Methods

LVs production and titration

The m*Galc* plasmid was obtained by inserting the mCherry sequence [(mCherry Monomeric derivative of DsRed fluorescent protein; sequence author: Clontech (TaKaRa); https://www.snapgene.com/resources/plasmidfiles/?set=fluorescent_protein_genes_and_plasmids&plasmid=mCherry)] downstream of the murine *Galc* cDNA[51] using the linker TRTRPLE.[40] The chimeric IDSsp.mGALC.APO enzyme was obtained from the m*Galc* as previously described.[40]

The chimeric IDUAsp.mGALC.APO enzyme was obtained from the m*Galc* by i) replacing the GALCsp (MANSQPKASQQRQAKVMTAAAGSASRVAVPLLLCALLVPGGA) with the IDUAsp (IMRPLRPRAALLALLASLLAAPPVAPAE); ii) adding a tandem repeat of the ApoE II receptor-binding region (APO), from amino acid 141 to 149 (APO: LRKLRKRLL LRKLRKRLL) downstream of the mCherry sequence using a flexible linker (LGGGGSGGGGSGGGGSGGGGS), as described.[37]

The chimeric hGALC enzymes were obtained from the codon-optimized human *GALC* (h*GALC*) sequence[32] by i) replacing the GALCsp (MTAAAGSAGRAAVPLLLCALLAPGGA) with the IDSsp (MPPPRTGRGLLWLGLVLSSVCVALG) or IDUAsp (MRPLRPRAALLALLASLLAAPPVAPAE); ii) adding the APO sequence, as described above for the murine enzyme.

The plasmids coding for murine (IDUAsp.m*Galc*.APO) and human (h*GALC*, IDSsp.h*GALC*.APO, IDUAsp.h*GALC*.APO) GALC enzymes were synthesized by Gene Script (Piscataway, New Jersey, USA). The m*Galc* and IDSsp.m*Galc*.APO constructs used for *in vitro* and *in vivo* experiments have been previously described.[40] Transgene expression was driven by the human phosphoglycerate kinase (hPGK) promoter. For the human construct, we utilized the lentiviral backbone from the HSPC-GT clinical trial for MPSI,[25] replacing the IDUA sequence with codon-optimized native and chimeric h*GALC* sequences. The substitutions were performed using EcoRI-HF and SalI-HF restriction enzymes (NEB, New England Biolabs, Ipswich, Massachusetts, USA) following the manufacturer's instructions. The LV expressing GFP under the hPGK promoter (LV.GFP) was used as a control.[77] VSV-pseudotyped third-generation LVs were produced by transient four-plasmid co-transfection into HEK293T cells and purified by ultracentrifugation, as described.[78,79] Expression titers and infectivity of vectors were assessed by quantitative droplet PCR (dd-PCR) as previously described[80] and reported in **Table S2**.

Cell isolation, culturing, and treatment

Cells were maintained in a 5% CO_2 humidified atmosphere at 37°C. Cells were transduced at the indicated multiplicity of infection (MOI) as calculated by titration of vector batches on HEK293T cells and expressed as transducing units (TU)/HEK293T cell.[80]

Isolation and LV transduction of murine HSPCs

Murine HSPCs were purified from the bone marrow (BM) of TWI and WT adult mice (30-40 days) by Lin^- selection using the mouse Lineage Cell Depletion Kit (Miltenyi Biotec, Bergisch Gladbach, Germany) according to the manufacturer's instructions. Cells were plated and transduced with LVs (MOI 100 for 12 hours) as described.[40] After 10 days, we counted the number of colonies (CFC assay) and collected the bulk pellets for VCN analysis. After 14 days of culture, the LC pellet and sup were collected for VCN, enzymatic activity, WB, IF, and Imagestream analyses. LC sup were collected for cross-correction experiments.

Differentiation of murine NSPCs into neurons/glia and cross-correction experiments

We established independent NSPC lines from TWI and WT mice as previously described.[81,82] Serially-passaged neurospheres were dissociated, and single cells were plated (4E+04 cells/cm^2) onto Matrigel (Corning, Bedford, Massachusetts, USA)-coated wells in complete medium, as described in.[82] After 2 days, we exposed them to fibroblast growth factor 2 (FGF2, Tebubio, Île-de-France, France)-containing medium (48 hours) and then to a mitogen-free medium added with fetal bovine serum (FBS - EuroClone, Milan, Italy) for 5 days, to promote neuronal and glial differentiation.[40] In the last 3 days of differentiation, TWI neuronal/glial cells were exposed every 24 hours to the sup of donor cells, namely UT WT HSPCs or LV-transduced TWI HSPCs (LC). XC cells, UT WT, and TWI controls were collected for GALC intracellular enzymatic activity and ELISA analyses.

Murine bEND.3 cells

bEND.3 cells (immortalized brain endothelioma murine cell line) were cultured in Dulbecco's modified eagle medium (DMEM– high glucose, Sigma-Aldrich, St. Louise, Missouri, USA), supplemented with 10% FBS, 1% penicillin/streptomycin (P/S, Lonza, Basel, Switzerland), and 1% Glutamine (Sigma-Aldrich), at the density of 5E+05 cells/cm^2. Adherent cells were detached using 0.25% trypsin-4 mM Ethylenediaminetetraacetic acid (EDTA) solution (Thermo Fisher Scientific, Waltham, Massachusetts, USA). The cell culture medium was replaced every 2 days. bEND.3 cells were plated onto 150 µg/mL collagen-coated transwell membranes (12mm Ø inserts, pore size 3.0 µm, growth area 1.12 cm^2 - COSTAR, Corning, Tewksbury, Massachusetts, USA) as described[83] for the

analyses of GALC transcytosis. Permeability studies to assess the optimal conditions ensuring cell confluency were performed using 4 kDa Fluorescein isothiocyanate–dextran (FD4, 200 µg/mL, Sigma-Aldrich; 30 minutes of incubation at 37°C) as described.[83] The fluorescence of the liberated molecule was measured with a spectrofluorometer (λ excitation 485 nm, λ emission 535 nm).

Human CD34$^+$ HSPC transduction

BM or G-colony-stimulating factor (G-CSF) mobilized peripheral blood (mPB) human CD34$^+$ cells (clinical protocol: Tiget05) were purchased from Lonza (Basel, Switzerland) and plated at 1E+05 cells/cm^2 in Retronectin (Takara Bio, San Jose, USA)-treated plates in serum-free StemSpan medium (StemCell Technologies, Vancouver, Canada) supplemented with P/S, recombinant human stem cell factor (rhSCF), recombinant human thrombopoietin (rhTPO), recombinant human Flt3 ligand (rhFlt3), and recombinant human IL6 (rhIL6) (all from PeproTech, Cranbury, USA) 22 ± 2 hours before transduction. Cyclosporine H (Sigma-Aldrich) was added to LV transduction media and maintained for 14±1 hours, as described.[55] HSPCs were washed, counted, and plated for the CFC assay (3E+02 - 4E+02 cells/ml in human Methocult - StemCell Technologies, Vancouver, Canada) or to obtain liquid cultures in Iscove's modified Dulbecco's medium (IMDM, Corning) supplemented with P/S, human cytokine (rhSCF by Miltenyi Biotec, rhIL3 and rhIL6 by PeproTech), 10% FBS (LC medium). LCs were counted every two days and plated at 1E+05 cells/cm^2 in the LC medium. After 14 days of culture, pellets and sup were collected for VCN, enzymatic activity, and WB analyses. After 14 days, CFCs were counted, and the bulk pellets were collected for VCN and FACS analyses. Sup from LC was collected for cross-correction experiments.

Human CD14$^+$ -derived macrophages

Human CD14$^+$ monocytes were purified from PB mononuclear cells of HD (n=3) and a late infantile GLD patient (n=1) using CD14 MicroBeads (Miltenyi Biotec), according to the manufacturer's instructions. To obtain macrophages, monocytes were plated in RPMI 1640 (Thermo Fisher Scientific) supplemented with FBS, P/S, human serum (EuroClone), and L-glutamine (Sigma-Aldrich) in the presence of human recombinant macrophage colony-stimulating factor (M-CSF, Miltenyi Biotec), as previously described.[56] For transduction, monocytes were incubated for 2 hours with the accessory viral protein vpl-VPX (4µl/1E+06 cells),[84] followed by overnight transduction at the MOI of 5. Viral-containing sup was removed, and cells were incubated with a growth medium for 9 days (M0 phenotype). Pellet and sup were collected for VCN and GALC enzymatic activity analyses. Sup from macrophages was collected for cross-correction experiments.

Human iPSCs and neuronal/glial differentiation

We induced neural differentiation of HD and GLD hiPSCs using a dual-Smad inhibition method.[85] iPSC colonies were detached with ACCUTASE (Sigma-Aldrich) and plated as single cells on Matrigel-coated dishes in StemMACS™ iPS-Brew XF medium (Miltenyi Biotec) with ROCK inhibitor Y-27632 (Sigma-Aldrich). After reaching 90% confluence, we switched to knockout serum replacement medium (Invitrogen, Waltham, Massachusetts, USA) with Noggin (R&D Systems, Minneapolis, Minnesota, USA) and SB431542 (Sigma-Aldrich) for 4 days, followed by a gradual transition to N2 medium with Noggin and SB431542. iPS-derived-NSPCs were expanded in N2 medium with bFGF, EGF (PeproTech), and ROCK inhibitor (Sigma-Aldrich). NPCs at passages 2-3 were detached and plated on Matrigel-coated dishes in the same medium for differentiation. N2 medium was gradually replaced with Glial Differentiation Medium (GDM) containing PDGF-AA, NT3, IGF-1, HGF (PeproTech), and T3 (Sigma-Aldrich). From day 14 onwards, cells were maintained in Glial Maturation Medium (GMM) with ascorbic acid, excluding growth factors, as described.[57,85] iPSCs, iPSC-derived NPCs, and differentiated progeny were maintained in a humidified atmosphere with 5% O_2 and 5% CO_2 at 37°C. In the last 24 hours of differentiation, GLD differentiated cells were exposed to the sup of donor cells (UT HD or LV-transduced HD $CD34^+$ progeny; UT HD, GLD, or LV-transduced macrophages). XC cells and UT HD and GLD controls were analyzed for GALC intracellular enzymatic activity assays and dosage of psychosine (by mass spectrometry, service outsourced to Laboratory for Genetic Metabolic Diseases, Academic Medical Center, University of Amsterdam).

Analyses of GALC transcytosis using bEND.3 cells in a transwell system

bEND.3 cells were plated onto collagen-coated Transwell membranes as described previously. After quantifying mGALC and IDUAsp.mGALC.APO in the donor sup (by mCherry ELISA assay; Abcam, Cambridge, UK), an equal amount of GALC-enriched medium was used in the subsequent experiments. PBS was added to the lower chamber of the transwell, while the GALC-enriched medium was added to the upper chamber. Transcytosis of GALC to the basolateral chamber was assessed by mCherry ELISA assay after 24 hours of incubation in a 5% CO_2 humidified atmosphere at 37°C.

Quantification of VCN

We isolated genomic DNA (gDNA) from cellular pellets and pellets from the bone marrow of treated mice using the Qiagen mini or micro kit (Qiagen, Hilden, Germany) or from the spleen of mice using the Maxwell RSC tissue

588 DNA kit (Promega, Madison, Wisconsin, USA) and the Maxwell RSC48 instrument (Promega), following the
589 provided instructions. DNA was quantified using the NanoDrop ND-1000 Spectrophotometer by measuring the
590 optical density at 260/280 nm. The VCN was assessed using quantitative droplet digital PCR (dd-PCR), following
591 the method outlined in.[80]
592
593 **Total mRNA extraction and RT-PCR**
594 Following the instructions, we extracted total RNA from cellular pellets using the RNeasy mini or micro Kit (Qiagen).
595 RNA quantification was performed with the NanoDrop ND-1000 Spectrophotometer. Following the manufacturer's
596 protocols, reverse transcription was conducted with 1 µg of total RNA and the QuantiTect Reverse Transcription
597 Kit (Qiagen).
598 qPCR was performed as previously described.[40] The probe and primers (TaqMan Gene Expression Assays,
599 Applied Biosystems, Waltham, Massachusetts, USA) are listed below:
600 Endogenous human *GALC*: Hs01012300_m1
601 Exogenous h*GALC* FW: GCGGAAGATGCTGAACTACC
602 Exogenous h*GALC* REV: GTGAAGTACTCGAACACGCC
603
604 **GALC activity assay**
605 GALC activity was assessed in cells, culture media, serum, and tissues as described.[86]
606
607 **Immunofluorescence**
608 IF analysis was conducted on cultured murine, human cells, and mouse tissues following established protocols.[40,87]
609 Primary and secondary antibodies utilized are detailed in **Table S3**. Confocal images were acquired at 4, 20, 40,
610 or 63X magnification using a Leica TCS SP8 confocal microscope (Leica, Wetzlar, Germany) or Mavig RS-G4
611 confocal microscope (MAVIG Research, Munich, Germany) and analyzed using LasX (Leica Application Suite X,
612 RRID: SCR_013673) or Imaris (Oxford Instruments, Abingdon-on-Thames, UK) software, respectively. Images
613 were imported into ImageJ or Adobe Photoshop 2021 to adjust brightness, contrast, and merge channels.
614
615 **Western Blot**
616 Cell pellets and tissues were resuspended in 50-200 µl (for cells) or 500 µl (for tissues) of radioimmunoprecipitation
617 assay (RIPA) lysis buffer enriched with protease (cOmplete Tablets, Roche, Basilea, Svizzera) and phosphatase

(PhosSTOP, Roche) inhibitors. Tissues underwent lysis using a homogenizer. Protein extraction was performed as previously described.[40] Protein concentration was determined using the DC Protein Assay (Biorad, Hercules, California, USA) and the MultiskanTM Go Microplate Spectrophotometer (Thermo Fisher Scientific). Proteins from the sup of cultures plated at the same cell density were obtained as previously described.[40] SDS-PAGE was employed to fractionate 5-15 µg of protein from the cell pellet and sup using NuPAGE™ 4-12% BisTris Protein Gels (Invitrogen), followed by transfer to nitrocellulose (NC) or polyvinylidene difluoride (PVDF) membranes (Invitrogen) using the iBlot2 Gel Transfer Device (Invitrogen). Proteins were transferred to PVDF membranes (Millipore, Burlington, USA) for 2 hours at 400mA to detect native and chimeric hGALC. We used the protein marker PM 2610 (Smobio). Immunodetection was performed using ClarityTM ECL Western Blotting Substrate (Biorad) and imaged with the Alliance Western Blot Imaging System (UVItec Limited, Cambridge, UK). Quantification of WB was conducted using ImageJ software, following the guidelines outlined in section 30.13 of the ImageJ User Guide version 1.46.

Imagestream

LV.IDUAsp.m*Galc*.APO-transduced TWI HSPCs (LC; 3E+06 cells) were stained and analyzed as previously described.[40] At least 2E+05 events were collected at 60X magnification, and approximately 8E+04 cells were analysed. The presence or absence of at least one overlapping mask (proximity or co-localization mask) was quantified.

ELISA for mCherry detection

Following instructions, quantitative measurement of mCherry protein in cell culture sup and cell extract samples was performed through the mCherry SimpleStep ELISA kit (Abcam). Neuronal/glial cells were lysed directly into the well in 70 µl of 1X cell extraction buffer PTR. Lysates were collected, incubated on ice for 15 minutes, and centrifuged at 16,000 x g at 4°C for 15 minutes. Protein concentration was determined using the DC Protein Assay (Biorad) and the MultiskanTM Go Microplate Spectrophotometer (Thermo Fisher Scientific). 3 µg of protein was used for mCherry detection.

Psychosine dosage

Galactosylsphingosine (LysoGalCer; psychosine) was quantified in treated and UT neural cells derived from induced pluripotent stem cells (iPSCs) from patients with GLD and HD as controls. The analytical procedure was

adapted from previously described protocols for glycosphingolipid and lysosphingolipid quantification in plasma and serum.[88,89,90] Cell pellets were homogenized in 150 µL of water by sonication on ice. A 50 µL aliquot was taken to determine protein concentration using the DC Protein Assay. For lipid extraction, 75 µL of homogenate was mixed with internal standards of 25 pmol LysoGalCer-d7 (25 µL, 1 µM in methanol). Subsequently, 240 µL of methanol and 150 µL of chloroform were added. After vortexing and incubation at RT, samples were centrifuged at 15,700 g for 10 minutes at 4°C to precipitate protein. The sup was transferred to a 2 mL tube, and 150 µL of chloroform and ammonium formate/formic acid buffer (225 µL, pH 3.15) were added. After vortexing, samples were centrifuged at 15,700 g for 3 minutes at 4°C to separate phases, and the upper phase was dried under nitrogen at 40°C. After butanol/water partitioning, the upper phase was again dried and reconstituted in 100 µL mobile phase B (95:5 acetonitrile: water with 1 mM ammonium formate and 0.1% formic acid). The lower phase (glycosphingolipids) was dried under nitrogen and subjected to deacylation by incubation with 0.5 mL 0.1 M NaOH in methanol using a microwave program. After neutralization with 50 µL 0.1 M HCl in methanol, the processed samples were combined with the lysosphingolipid workflow from the drying step. UPLC-MS/MS analysis was performed on a Waters Acquity UPLC system coupled to a Waters Xevo TQ-XS mass spectrometer, operating in positive electrospray ionization (ESI) mode. Chromatographic separation was achieved on an Ascentis® Express HILIC column (4.6 × 50 mm, 2.7 µm, Supelco) with a HILIC Securityguard™ precolumn (4 × 3.0 mm, Phenomenex) at room temperature. The mobile phases consisted of (A) water with 1 mM ammonium formate and 0.1% formic acid, and (B) acetonitrile/water (95:5) with 1 mM ammonium formate and 0.1% formic acid. A gradient elution was applied at 1.5 mL/min with the following program: 0–0.2 min, 100–95% B; 0.2–3.5 min, 95% B; 3.5–4.0 min, 95–10% B; 4.0–5.0 min, 10% B; 5.0–5.1 min, 10–100% B; 5.1–7.0 min, 100% B. The injection volume was 10 µL. Analytes of specific mass transitions were detected using multiple reaction monitoring (MRM). Quantification was performed against matrix-matched calibration curves using deuterated internal standards. Data acquisition and processing were carried out using MassLynx software. Psychosine concentration was normalized to the protein content of the homogenate and expressed as pmol per gram of protein.

Mice

NOD.Cg-PrkdcscidIL2rgtm1Wjl/SzJ (NSG), transgenic CAG-GFP (TgCAG-GFP, background C57BL/6-Tg (CAGeGFP1Osb/J) and TWI mice were purchased from The Jackson Laboratory (Bar Harbor, Maine, USA). Mouse colonies are maintained in the animal facility of the San Raffaele Scientific Institute, Milano, Italy.

677 ***In vivo* treatments**

678

679 Myeloablative regimen

680 Between 16 and 24 hours before transplantation, neonatal (PND 1-2) TWI and WT pups of both sexes underwent
681 conditioning either with sublethal TBI at 400 cGy or received a single intraperitoneal injection of 20 mg/kg of BUS
682 (Busilvex 6 mg/ml, Pierre Fabre, Boulogne-Billancourt, France). UT, TWI, and WT littermates were utilized as the
683 control group. Female NSG mice aged eight to ten weeks were conditioned with sublethal TBI at 180 cGy as
684 described.[55] Conditioned mice were given Gentamycin (final concentration 320 mg/mL, Italfarmaco, Milan, Italy)
685 in their drinking water starting from the day of conditioning for the subsequent 2 months.

686

687 Total bone marrow transplant

688 Four to eight-week-old TgCAG-GFP mice were used as donors and euthanized using CO_2. BM from their tibias
689 and femurs was flushed out with PBS and centrifuged at 500 x g for 5 minutes. Red blood cells in the BM pellet
690 were lysed with double-distilled water (ddH2O) for 10 seconds, and the reaction was stopped by adding PBS with
691 10% FBS. The cell suspension was then filtered through a 40 µm cell strainer (BD Biosciences, New Jersey, USA)
692 and centrifuged at 500 x g for 5 minutes. The cells were resuspended in PBS (5E+06 cells/50 µL) and immediately
693 injected into myeloablated recipient mice. The donor BM cells expressed GFP and had physiological GALC activity
694 levels. Neonatal receiver mice (PND 2-3) were briefly anesthetized on ice for 1 minute to induce transient
695 hypothermia. The donor cells were injected into the temporal vein using a U-100 insulin syringe (DB Micro-Fine,
696 0.3 ml). After injection, the pups were warmed under a heat lamp for approximately 1 minute. The entire procedure
697 took less than 3 minutes per mouse, after which the neonates were promptly returned to their parental cages. The
698 survival rate after the procedure exceeded 95%. Experimental animals of both sexes were randomly assigned to
699 groups before determining their sex. Untreated TWI and WT littermates were included as controls. No differences
700 in treatment outcomes based on sex were observed.

701

702 HSPC gene therapy

703 HSPCs (Lin^- cells) from WT and TWI mice were isolated as previously described.[80] The day after transduction with
704 different vectors (LV.GFP at 50 MOI; LV.m*Galc* and LV.IDUAsp.m*Galc*.APO at 100 MOI), the HSPCs were
705 suspended in PBS (5E+05 cells/50 µL) and immediately injected using a U-100 insulin syringe (DB Micro-Fine,
706 0.3 ml) into the temporal vein of myeloablated recipient mice as described above. Experimental animals of both

sexes were randomly assigned to groups before determining their sex. Untreated TWI and WT littermates were included as controls. No differences in treatment outcomes based on sex were observed.

Xenotransplantation of human HSPCs

CD34$^+$ HSPCs derived from HD were transduced with LV.h*GALC*, LV.IDUAsp.h*GALC*.APO and LV.GFP as control at 100 MOI. Conditioned NSG female mice were intravenously transplanted via retroorbital injection or tail vein with 3-5E+05 cells in a 100-150 µL PBS suspension using a U-100 insulin syringe (DB Micro-Fine, 0.3 ml).

Tissue collection and processing

Treated and control mice were anesthetized with Ketamine-Xylazine (from SIGMA, 100 and 10 mg/Kg, respectively) and intracardially perfused via the descending aorta with 0.9% NaCl + 25,000 heparin sodium I.U./ml (PharmaTex, Italy, Milan). Brain, spinal cord, sciatic nerve, liver, spleen, and BM tissues were collected for enzymatic activity. The two brain hemispheres were separated, and each hemisphere was again divided into two parts. An integral hemisphere was used for IF analysis and to freshly isolate CD45$^+$ and CD45$^-$ cell populations. For the other, a cut was made, thus separating the rostral region (RO), comprising the telencephalon, diencephalon, and midbrain; the caudal region (CA), comprising the cerebellum, pons, and medulla. The RO and CA regions were analysed for WB and pooled to analyse the GALC enzymatic activity. The spinal cord was collected as a whole and then sagittally halved. The BM was collected as described above and immediately frozen for subsequent enzymatic activity and VCN analyses. For IF analysis, sections of the brain and spinal cord tissues were fixed for 24 hours in 4% paraformaldehyde (PFA, Santa Cruz Biotechnology, Dallas, Texas, USA) and included in 4% agarose (EuroClone) as already reported.[87] Serial coronal vibratome sections (6 series, 40 µm-thick) were stained as described above. For biochemical and molecular assays, tissues were quickly frozen in liquid nitrogen.

Adult brain dissociation

CD45$^+$ myeloid cells and a mixed CD45$^-$ cell population, consisting of neuronal, glial, and endothelial cells, were freshly isolated using the Adult Brain Dissociation Kit (Miltenyi Biotec) according to the manufacturer's protocol. CD45$^+$ and CD45$^-$ cell fractions were subsequently analyzed for cytofluorimetric and GALC enzymatic activity analyses.

736

737 **Cytofluorimetric analyses**

738 Cell composition of LV-transduced CD34$^+$ progeny

739 2E+05 cells from the LC and CFC bulk were incubated in FACS buffer (PBS, 5% FBS, 1% BSA) for 15 minutes.
740 After incubation for 30 minutes at 4°C with antibodies (listed in **Table S3**), cells were centrifuged at 500 x g for 5
741 minutes and resuspended in FACS buffer as already described.[91]

742

743 Engraftment and composition of donor-derived cells in treated mice

744 PB and BM were collected from treated and untreated mice. The spleen collected from UT and treated NSG mice
745 was smashed through a cell strainer (40 µm) in PBS. The CD45$^+$ and CD45$^-$ cell populations were freshly isolated
746 from the brains of tBM-T and UT mice as described above. 1-2E+05 cells or 20 µl of PB of each sample were
747 incubated for 30 minutes at 4°C with antibodies (listed in **Table S3**). The GFP and mCherry signals were measured
748 by direct fluorescence. The PB samples were incubated for 15 minutes on ice with 1 mL of ammonium-chloride-
749 potassium (ACK, Thermo Fisher Scientific) buffer for red blood cell lysis, following the manufacturer's instructions.
750 Samples were centrifuged at 800 x g for 5 minutes and resuspended in FACS buffer. Cell suspensions were
751 analyzed using a flow cytometer (Canto II, BD Biosciences, Franklin Lakes, NJ, USA; Cytoflex, Beckman Coulter,
752 Brea, California, USA). Data were analysed using the FlowJo software.

753

754 **Statistics**

755 Data were analysed with GraphPad Prism version 10.0 for Macintosh and expressed as the mean or mean ± SD
756 standard deviation (SD) when n≥2. One-way ANOVA or Kruskal-Wallis followed by appropriate post-tests and
757 unpaired t-test or Mann-Whitney tests were used. Correlation analysis was performed using Spearman's
758 correlation. Survival curves were analysed using the log-rank (Mantel-Cox) test. The P-value threshold for
759 statistical significance was considered 0.05. The number of samples and statistical tests used are indicated in the
760 figure legends.

761

762 **Data availability statement**

763 The data for this publication are available upon request to scientific community members for research purposes.

764

Acknowledgements

We are grateful to Luigi Tiradani and Francesca Ornaghi for vector preparation and titration, Vasco Meneghini, Filippo Casalini and Ilaria Laface for help in CD14$^+$ cell culture and differentiation, Tiziano Di Tomaso for assistance with the cloning strategy, Bernhard Gentner for providing the LV backbone, Alessandra Biffi for providing the codon-optimized h*GALC* cDNA, Janet E. Deane for providing the anti-hGALC antibody, Desirèe Zambroni for the ImageStream analysis, Valeria Berno and Cesare Covino for confocal microscopy support, Alessandro Nonis (University Centre of Statistics in Biomedical Sciences – CUSSB, Vita-Salute San Raffaele University) for support with the statistical analysis, Frèdéric M. Vaz (University of Amsterdam) for psychosine analysis, all the members of the Gritti's lab for continuous support and helpful discussion. Part of this work was carried out in ALEMBIC (Advanced Light and Electron Microscopy BioImaging Center) and FRACTAL (Flow Cytometry Resource, Advanced Cytometry Technical Applications Laboratory), the core facilities established at IRCSS Ospedale San Raffaele and Vita-Salute San Raffaele University.

All animal procedures were performed according to protocols approved by the 'Institutional Committee for the Good Animal Experimentation' of the San Raffaele Scientific Institute (IACUC #791, IACUC #1145, and IACUC #1192) and are reported to the Ministry of Health, as required by Italian law.

Human cells were used according to the guidelines on human research issued by the ethics committee of Ospedale San Raffaele in the context of the protocols TIGET-HPCT, Tiget05 (GR-2019-12369357), Tiget09 (GR2019-microMLD, 12368930).

This study was funded by grants from Fondazione Telethon (TTAGD0222TT) to A.G., ELA 2019-015I2 to A.G., Italian Ministry of Health (GR-2019-12369357) to A.R (PI), A.K.R (co-PI) and F.M., FONDAZIONE CENTRO SAN RAFFAELE (FCSR)-2019 fellowship program to F.C; The sponsor(s) had no role in the study design, data collection, analysis, and interpretation or the decision to submit the article for publication; F.C. conducted part of this study to fulfill his PhD in Molecular Medicine, XXXV cycle (Vita-Salute San Raffaele University) with the support of fellowships co-funded by Ministero dell'Istruzione e del Merito (MIUR) and Vita-Salute San Raffaele University.

Author Contributions

F.C. and A.R. contributed to the conception and design of the study, wrote the manuscript, and performed the statistical analysis; F.C., A.R., I.P., M.F., and V.S. performed *in vitro* and *in vivo* experiments; E.V. and G.U. performed the *in vitro* experiments on CD34$^+$ HSPCs; S.M. supervised the biochemical analyses; F.M. performed

794 the biochemical analyses; A.K.R. provided expertise, resources, and intellectual input; A.G. designed and
795 supervised the study, provided resources, wrote the manuscript, and approved the final version. All authors
796 contributed to the manuscript revision and read and approved the submitted version.
797
798 **Declaration of interests statement**
799 The authors declare that the research was conducted without any commercial or financial relationships that could
800 be construed as a potential conflict of interest.
801
802 **Keywords**
803 Globoid cell leukodystrophy, chimeric enzymes, hematopoietic stem/progenitor cells, gene therapy, lentiviral
804 vectors, cross-correction

References

1. Ketata, I., and Ellouz, E. (2024). From pathological mechanisms in Krabbe disease to cutting-edge therapy: A comprehensive review. Neuropathology. Aug;44(4):255-257.
2. Orsini, J.J., Escolar, M.L., Wasserstein MP, Caggana, M. Krabbe Disease. (2000). In: Adam MP, Feldman J, Mirzaa GM, Pagon RA, Wallace SE, Amemiya A, editors. GeneReviews® [Internet]. Seattle (WA): University of Washington, Seattle; 1993–2025.
3. Lee, W.C., Courtenay, A., Troendle, F.J., Stallings-Mann, M.L., Dickey, C.A., Delucia, M.W., Dickson, D.W., and Eckman, C.B. (2005). Enzyme replacement therapy results in substantial improvements in early clinical phenotype in a mouse model of globoid cell leukodystrophy. The FASEB J. Sep;19(11): 1549-51.
4. Matthes, F., Andersson, C., Stein, A., Eistrup, C., Fogh, J., Gieselmann, V., Wenger, D.A., and Matzner, U. (2015). Enzyme replacement therapy of a novel humanized mouse model of globoid cell leukodystrophy. Exp Neurol. Sep:271:36-45.
5. Grosso, A. Del, Galliani, M., Angella, L., Santi, M., Tonazzini, I., Parlanti, G., Signore, G., and Cecchini, M. (2019). Brain-targeted enzyme-loaded nanoparticles: A breach through the blood-brain barrier for enzyme replacement therapy in Krabbe disease. Sci Adv. Nov 20;5(11): eaax7462.
6. Escolar, M.L., Poe, M.D., Provenzale, J.M., Richards, K.C., Allison, J., Wood, S., Wenger, D.A., Pietryga, D., Wall, D., Champagne, M., et al. (2005). Transplantation of Umbilical-Cord Blood in Babies with Infantile Krabbe's Disease. New England Journal of Medicine. May 19;352(20):2069-81.
7. Allewelt, H., Taskindoust, M., Troy, J., Page, K., Wood, S., Parikh, S., Prasad, V.K., and Kurtzberg, J. (2018). Long-Term Functional Outcomes after Hematopoietic Stem Cell Transplant for Early Infantile Krabbe Disease. Biology of Blood and Marrow Transplantation. Nov; 24(11):2233-2238.
8. Duffner, P.K., Caviness, V.S., Erbe, R.W., Patterson, M.C., Schultz, K.R., Wenger, D.A., and Whitley, C. (2009). The long-term outcomes of presymptomatic infants transplanted for Krabbe disease: Report of the workshop held on July 11 and 12, 2008, Holiday Valley, New York.Genet Med. June;11(6):450-4
9. Kofler, J., Beltran-Quintero, M.L., Rugari, A., Zuccoli, G., Klotz, S., and Escolar, M.L. (2022). Improved Brain Pathology and Progressive Peripheral Neuropathy in a 15 Year Old Survivor of Infantile Krabbe Disease Treated With Umbilical Cord Transplantation. Front Mol Neurosci. Jul 28:15:888231.
10. Solomon, M., and Muro, S. (2017). Lysosomal enzyme replacement therapies: Historical development, clinical outcomes, and future perspectives. Adv Drug Deliv Rev. Sep 1:118:109-134.
11. Lugt, M.T.V., Chen, X., Escolar, M.L., Carella, B.A., Barnum, J.L., Windreich, R.M., Hill, M.J., Poe, M., Marsh, R.A., Stanczak, H., et al. (2020). Reduced-intensity single-unit unrelated cord blood transplant with optional immune boost for nonmalignant disorders. Blood Adv. Jul 14;4(13):3041-3052.
12. Xu, Z.L., and Huang, X.J. (2021). Optimizing allogeneic grafts in hematopoietic stem cell transplantation. Stem Cells Transl Med. Nov;10 Suppl 2(Suppl 2):S41-S47.
13. Bradbury, A.M., Rafi, M.A., Bagel, J.H., Brisson, B.K., Marshall, M.S., Pesayco Salvador, J., Jiang, X., Swain, G.P., Prociuk, M.L., Odonnell, P.A., et al. (2018). AAVrh10 Gene Therapy Ameliorates Central and Peripheral Nervous System Disease in Canine Globoid Cell Leukodystrophy (Krabbe Disease). Hum Gene Ther. Jul;29(7):785-801.
14. Hordeaux, J., Jeffrey, B.A., Jian, J., Choudhury, G.R., Michalson, K., Mitchell, T.W., Buza, E.L., Chichester, J., Dyer, C., Bagel, J., et al. (2022). Efficacy and Safety of a Krabbe Disease Gene Therapy. Hum Gene Ther. May;33(9-10):499-517.
15. Rafi, M.A., Rao, H.Z., Luzi, P., Curtis, M.T., and Wenger, D.A. (2012). Extended normal life after AAVrh10-mediated gene therapy in the mouse model of krabbe disease. Molecular Therapy. Nov;20(11):2031-42.
16. Li, Y., Miller, C.A., Shea, L.K., Jiang, X., Guzman, M.A., Chandler, R.J., Ramakrishnan, S.M., Smith, S.N., Venditti, C.P., Vogler, C.A., et al. (2021). Enhanced Efficacy and Increased Long-Term Toxicity of CNS-Directed, AAV-Based Combination Therapy for Krabbe Disease. Molecular Therapy. Feb 3;29(2):691-701.
17. Hordeaux, J., Lamontagne, R.J., Song, C., Buchlis, G., Dyer, C., Buza, E.L., Ramezani, A., Wielechowski, E., Greig, J.A., Chichester, J.A., et al. (2024). High-dose systemic adeno-associated virus

vector administration causes liver and sinusoidal endothelial cell injury. Molecular Therapy. Apr 3;32(4):952-968.

18. Sabatino, D.E., Bushman, F.D., Chandler, R.J., Crystal, R.G., Davidson, B.L., Dolmetsch, R., Eggan, K.C., Gao, G., Gil-Farina, I., Kay, M.A., et al. (2022). Evaluating the state of the science for adeno-associated virus integration: An integrated perspective. Mol Ther. Aug 3;30(8):2646-2663.
19. Calabria, A., Cipriani, C., Spinozzi, G., Rudilosso, L., Esposito, S., Benedicenti, F., Albertini, A., Pouzolles, M., Luoni, M., Giannelli, S., et al. (2023). Intrathymic AAV delivery results in therapeutic site-specific integration at TCR loci in mice. Blood. May 11;141(19):2316-2329.
20. Lek, A., Wong, B., Keeler, A., Blackwood, M., Ma, K., Huang, S., Sylvia, K., Batista, A.R., Artinian, R., Kokoski, D., et al. (2023). Death after High-Dose rAAV9 Gene Therapy in a Patient with Duchenne's Muscular Dystrophy. New England Journal of Medicine. Sep 28;389(13):1203-1210.
21. Nisanov, A.M., de Jesús, J.A., and Schaffer, D. V (2025). Advances in AAV capsid engineering: Integrating rational design, directed evolution and machine learning. Mol Ther. May 7;33(5):1937-1945.
22. Park, M.T., Verma, A., Froelich, C.A., and Motevalian, S.P. (2025). Process and quality considerations for recombinant adeno-associated virus manufacturing platforms. Trends Biotechnol. Mar 27:S0167-7799(25)00079-4.
23. Biffi, A., Capotondo, A., Fasano, S., Del Carro, U., Marchesini, S., Azuma, H., Malaguti, M.C., Amadio, S., Brambilla, R., Grompe, M., et al. (2006). Gene therapy of metachromatic leukodystrophy reverses neurological damage and deficits in mice. Journal of Clinical Investigation. Nov;116(11):3070-82.
24. Capotondo, A., Milazzo, R., Politi, L.S., Quattrini, A., Palini, A., Plati, T., Merella, S., Nonis, A., Di Serio, C., Montini, E., et al. (2012). Brain conditioning is instrumental for successful microglia reconstitution following hematopoietic stem cell transplantation. Proc Natl Acad Sci U S A. Sep 11;109(37):15018-23.
25. Gentner, B., Tucci, F., Galimberti, S., Fumagalli, F., De Pellegrin, M., Silvani, P., Camesasca, C., Pontesilli, S., Darin, S., Ciotti, F., et al. (2021). Hematopoietic Stem- and Progenitor-Cell Gene Therapy for Hurler Syndrome. New England Journal of Medicine. Nov 18;385(21):1929-1940.
26. Montini, E., Naldini, L., Booth, C., Kohn, D.B., and Aiuti, A. (2024). Balancing efficacy and safety in lentiviral vector-mediated hematopoietic stem cell gene therapy. Mol Ther. Jan 8;33(1):6-8.
27. Calabria, A., Spinozzi, G., Cesana, D., Buscaroli, E., Benedicenti, F., Pais, G., Gazzo, F., Scala, S., Lidonnici, M.R., Scaramuzza, S., et al. (2024). Long-term lineage commitment in haematopoietic stem cell gene therapy. Nature. Dec;636(8041):162-171.
28. Biffi, A., Montini, E., Lorioli, L., Cesani, M., Fumagalli, F., Plati, T., Baldoli, C., Martino, S., Calabria, A., Canale, S., et al. (2013). Lentiviral hematopoietic stem cell gene therapy benefits metachromatic leukodystrophy. Science. Aug 23;341(6148):1233158.
29. Suzuki, K., and Suzuki, K. (1995). The Twitcher Mouse: A Model for Krabbe Disease and for Experimental Therapies. Brain Pathology. Jul;5(3):249-58.
30. Taniike, M., Mohri, I., Eguchi, N., Irikura, D., Urade, Y., Okada, S., and Suzuki, K. (1999). An apoptotic depletion of oligodendrocytes in the twitcher, a murine model of globoid cell leukodystrophy. J Neuropathol Exp Neurol. Jun;58(6):644-53.
31. Gentner, B., Visigalli, I., Hiramatsu, H., Lechman, E., Ungari, S., Giustacchini, A., Schira, G., Amendola, M., Quattrini, A., Martino, S., et al. (2010). Identification of hematopoietic stem cell-specific miRNAs enables gene therapy of globoid cell leukodystrophy. Sci Transl Med. Nov 17;2(58):58ra84.
32. Ungari, S., Montepeloso, A., Morena, F., Cocchiarella, F., Recchia, A., Martino, S., Gentner, B., Naldini, L., and Biffi, A. (2015). Design of a regulated lentiviral vector for hematopoietic stem cell gene therapy of globoid cell leukodystrophy. Mol Ther Methods Clin Dev. Oct 14:2:15038.
33. Reddy, A.S., Kim, J.H., Hawkins-Salsbury, J.A., Macauley, S.L., Tracy, E.T., Vogler, C.A., Han, X., Song, S.K., Wozniak, D.F., Fowler, S.C., et al. (2011). Bone marrow transplantation augments the effect of brain- and spinal cord-directed adeno-associated virus 2/5 gene therapy by altering inflammation in the murine model of globoid-cell leukodystrophy. Journal of Neuroscience. Jul 6;31(27):9945-57.
34. Nagano, S., Yamada, T., Shinnoh, N., Furuya, H., Taniwaki, T., and Kira, J.I. (1998). Expression and processing of recombinant human galactosylceramidase. Clinica Chimica Acta. Aug 10;276(1):53-61.

35. Spratley, S.J., Hill, C.H., Viuff, A.H., Edgar, J.R., Skjødt, K., and Deane, J.E. (2016). Molecular Mechanisms of Disease Pathogenesis Differ in Krabbe Disease Variants. Traffic. Aug;17(8):908-22.
36. Biffi, A., De Palma, M., Quattrini, A., Del Carro, U., Amadio, S., Visigalli, I., Sessa, M., Fasano, S., Brambilla, R., Marchesini, S., et al. (2004). Correction of metachromatic leukodystrophy in the mouse model by transplantation of genetically modified hematopoietic stem cells. Journal of Clinical Investigation. Apr;113(8):1118-29.
37. Gleitz, H.F., Liao, A.Y., Cook, J.R., Rowlston, S.F., Forte, G.M., D'Souza, Z., O'Leary, C., Holley, R.J., and Bigger, B.W. (2018). Brain-targeted stem cell gene therapy corrects mucopolysaccharidosis type II via multiple mechanisms. EMBO Mol Med. Jul;10(7):e8730.
38. Visigalli, I., Delai, S., Ferro, F., Cecere, F., Vezzoli, M., Sanvito, F., Chanut, F., Benedicenti, F., Spinozzi, G., Wynn, R., et al. (2016). Preclinical Testing of the Safety and Tolerability of Lentiviral Vector-Mediated Above-Normal Alpha-L-Iduronidase Expression in Murine and Human Hematopoietic Cells Using Toxicology and Biodistribution Good Laboratory Practice Studies. Hum Gene Ther. Oct;27(10):813-829.
39. Visigalli, I., Ungari, S., Martino, S., Park, H., Cesani, M., Gentner, B., Sergi, L.S., Orlacchio, A., Naldini, L., and Biffi, A. (2010). The galactocerebrosidase enzyme contributes to the maintenance of a functional hematopoietic stem cell niche. Blood. Sep 16;116(11):1857-66.
40. Ricca, A., Cascino, F., Morena, F., Martino, S., and Gritti, A. (2020). In vitro Validation of Chimeric β-Galactosylceramidase Enzymes With Improved Enzymatic Activity and Increased Secretion. Front Mol Biosci. Jul 21:7:167.
41. Sorrentino, N.C., D'Orsi, L., Sambri, I., Nusco, E., Monaco, C., Spampanato, C., Polishchuk, E., Saccone, P., De Leonibus, E., Ballabio, A., et al. (2013). A highly secreted sulphamidase engineered to cross the blood-brain barrier corrects brain lesions of mice with mucopolysaccharidoses type IIIA. EMBO Mol Med. May;5(5):675-90.
42. Ellison, S., Liao, A., Gleitz, H.F.E., Parker, H., Booth, L., Robinson, J., Wood, S., Taylor, J., Holley, R., and Bigger, B.W. (2023). Sustained long-term disease correction in a murine model of MPSII following stem cell gene therapy. Mol Ther Methods Clin Dev. Oct 20:31:101127.
43. Zhang, X.Y., Dinh, A., Cronin, J., Li, S.C., and Reiser, J. (2008). Cellular uptake and lysosomal delivery of galactocerebrosidase tagged with the HIV Tat protein transduction domain. J Neurochem. Feb;104(4):1055-64.
44. Hu, P., Li, Y., Nikolaishvili-Feinberg, N., Scesa, G., Bi, Y., Pan, D., Moore, D., Bongarzone, E.R., Sands, M.S., Miller, R., et al. (2016). Hematopoietic Stem cell transplantation and lentiviral vector-based gene therapy for Krabbe's disease: Present convictions and future prospects. J Neurosci Res. Nov;94(11):1152-68.
45. Pan, X., Sands, S.A., Yue, Y., Zhang, K., Levine, S.M., and Duan, D. (2019). An Engineered Galactosylceramidase Construct Improves AAV Gene Therapy for Krabbe Disease in Twitcher Mice. Hum Gene Ther. Sep;30(9):1039-1054.
46. Knappskog, S., Ravneberg, H., Gjerdrum, C., Trösße, C., Stern, B., and Pryme, I.F. (2007). The level of synthesis and secretion of Gaussia princeps luciferase in transfected CHO cells is heavily dependent on the choice of signal peptide. J Biotechnol. Mar 10;128(4):705-15.
47. Kober, L., Zehe, C., and Bode, J. (2013). Optimized signal peptides for the development of high expressing CHO cell lines. Biotechnol Bioeng. Apr;110(4):1164-73.
48. Stern, B., Optun, A., Liesenfeld, M., Gey, C., Gräfe, M., and Pryme, I.F. (2011). Enhanced protein synthesis and secretion using a rational signal-peptide library approach as a tailored tool. BMC Proc. Nov 22;5 Suppl 8(Suppl 8):O13.
49. Zhang, L., Leng, Q., and Mixson, A.J. (2005). Alteration in the IL-2 signal peptide affects secretion of proteins in vitro and in vivo. Journal of Gene Medicine. Mar;7(3):354-65.
50. Spratley, S.J., and Deane, J.E. (2016). New therapeutic approaches for Krabbe disease: The potential of pharmacological chaperones. Nov;94(11):1203-19.
51. Neri, M., Ricca, A., Di Girolamo, I., Alcala'-Franco, B., Cavazzin, C., Orlacchio, A., Martino, S., Naldini, L., and Gritti, A. (2011). Neural stem cell gene therapy ameliorates pathology and function in a mouse model of globoid cell leukodystrophy. Stem Cells. Oct;29(10):1559-71.

52. Böckenhoff, A., Cramer, S., Wölte, P., Knieling, S., Wohlenberg, C., Gieselmann, V., Galla, H.J., and Matzner, U. (2014). Comparison of five peptide vectors for improved brain delivery of the lysosomal enzyme arylsulfatase A. Journal of Neuroscience. Feb 26;34(9):3122-9.
53. Santambrogio, S., Ricca, A., Maderna, C., Ieraci, A., Aureli, M., Sonnino, S., Kulik, W., Aimar, P., Bonfanti, L., Martino, S., et al. (2012). The galactocerebrosidase enzyme contributes to maintain a functional neurogenic niche during early post-natal CNS development. Hum Mol Genet. Nov 1;21(21):4732-50.
54. Ricca, A., Rufo, N., Ungari, S., Morena, F., Martino, S., Kulik, W., Alberizzi, V., Bolino, A., Bianchi, F., Del Carro, U., et al. (2015). Combined gene/cell therapies provide long-term and pervasive rescue of multiple pathological symptoms in a murine model of globoid cell leukodystrophy. Hum Mol Genet. Jun 15;24(12):3372-89.
55. Petrillo, C., Thorne, L.G., Unali, G., Schiroli, G., Giordano, A.M.S., Piras, F., Cuccovillo, I., Petit, S.J., Ahsan, F., Noursadeghi, M., et al. (2018). Cyclosporine H Overcomes Innate Immune Restrictions to Improve Lentiviral Transduction and Gene Editing In Human Hematopoietic Stem Cells. Cell Stem Cell. Dec 6;23(6):820-832.e9.
56. Zoccolillo, M., Brigida, I., Barzaghi, F., Scala, S., Hernandez, R.J., Basso-Ricci, L., Colantuoni, M., Pettinato, E., Sergi, L.S., Milardi, G., et al. (2021). Lentiviral correction of enzymatic activity restrains macrophage inflammation in adenosine deaminase 2 deficiency. Blood Adv. Aug 24;5(16):3174-3187.
57. Mangiameli, E., Cecchele, A., Morena, F., Sanvito, F., Matafora, V., Cattaneo, A., della Volpe, L., Gnani, D., Paulis, M., Susani, L., et al. (2021). Human iPSC-based neurodevelopmental models of globoid cell leukodystrophy uncover patient- and cell type-specific disease phenotypes. Stem Cell Reports. Jun 8;16(6):1478-1495.
58. Chen, Y.Q., Rafi, M.A., De Gala, G., and Wenger, D.A. (1993). Cloning and expression cDNA encoding human galactocerebrosidase, the enzyme deficient in globoid cell leukodystrophy. Hum Mol Genet. Nov;2(11):1841-5.
59. Luzi, P., Victoria, T., Rafi, M.A., and Wenger, D.A. (1997). Analysis of the 5' flanking region of the human galactocerebrosidase (GALC) gene. Biochem Mol Med. Dec;62(2):159-64.
60. Ferrari, G., Thrasher, A.J., and Aiuti, A. (2021). Gene therapy using haematopoietic stem and progenitor cells. Nat Rev Genet. Apr;22(4):216-234.
61. Tucci, F., Galimberti, S., Naldini, L., Valsecchi, M.G., and Aiuti, A. (2022). A systematic review and meta-analysis of gene therapy with hematopoietic stem and progenitor cells for monogenic disorders. Nat Commun. Mar 14;13(1):1315.
62. Plasschaert, R.N., DeAndrade, M.P., Hull, F., Nguyen, Q., Peterson, T., Yan, A., Loperfido, M., Baricordi, C., Barbarossa, L., Yoon, J.K., et al. (2022). High-throughput analysis of hematopoietic stem cell engraftment after intravenous and intracerebroventricular dosing. Molecular Therapy. Oct 5;30(10):3209-3225.
63. Sailor, K.A., Agoranos, G., López-Manzaneda, S., Tada, S., Gillet-Legrand, B., Guerinot, C., Masson, J.B., Vestergaard, C.L., Bonner, M., Gagnidze, K., et al. (2022). Hematopoietic stem cell transplantation chemotherapy causes microglia senescence and peripheral macrophage engraftment in the brain. Nat Med. Mar;28(3):517-527.
64. Shemer, A., Grozovski, J., Tay, T.L., Tao, J., Volaski, A., Süß, P., Ardura-Fabregat, A., Gross-Vered, M., Kim, J.S., David, E., et al. (2018). Engrafted parenchymal brain macrophages differ from microglia in transcriptome, chromatin landscape and response to challenge. Nat Commun. Dec 6;9(1):5206.
65. Yeager, A.M., Brennan, S., Tiffany, C., Moser, H.W., and Santos, G.W. (1984). Prolonged survival and remyelination after hematopoietic cell transplantation in the twitcher mouse. Science. Sep 7;225(4666):1052-4.
66. Rafi, M.A., Rao, H.Z., Luzi, P., and Wenger, D.A. (2015). Long-term improvements in lifespan and pathology in CNS and PNS after BMT plus one intravenous injection of AAVrh10-GALC in twitcher mice. Molecular Therapy. Nov;23(11):1681-1690.
67. Rafi, M.A., Luzi, P., and Wenger, D.A. (2020). Conditions for combining gene therapy with bone marrow transplantation in murine Krabbe disease. BioImpacts. 2020;10(2):105-115.

68. Azario, I., Pievani, A., Del Priore, F., Antolini, L., Santi, L., Corsi, A., Cardinale, L., Sawamoto, K., Kubaski, F., Gentner, B., et al. (2017). Neonatal umbilical cord blood transplantation halts skeletal disease progression in the murine model of MPS-I. Sci Rep. Aug 25;7(1):9473.
69. Jones, R.J., Wagner, J.E., Celano, P., Zicha, M.S., and Sharkis, S.J. (1990). Separation of pluripotent haematopoietic stem cells from spleen colony-forming cells. Nature. Sep 13;347(6289):188-9.
70. Zijlmans, J.M., Visser, J.W.M., Laterveer, L., Kleiverda, K., Heemskerk, D.P.M., Kluin, P.M., Willemze, R., and Fibbe, W.E. (1998). The early phase of engraftment after murine blood cell transplantation is mediated by hematopoietic stem cells. Proc Natl Acad Sci U S A. Jan 20;95(2):725-9.
71. Hohsfield, L.A., Najafi, A.R., Ghorbanian, Y., Soni, N., Crapser, J.D., Figueroa Velez, D.X., Jiang, S., Royer, S.E., Kim, S.J., Henningfield, C.M., et al. (2021). Subventricular zone/white matter microglia reconstitute the empty adult microglial niche in a dynamic wave. Elife. Aug 23:10:e66738.
72. Huang, Y., Xu, Z., Xiong, S., Sun, F., Qin, G., Hu, G., Wang, J., Zhao, L., Liang, Y.X., Wu, T., et al. (2018). Repopulated microglia are solely derived from the proliferation of residual microglia after acute depletion. Nat Neurosci. Apr; 21(4):530-540.
73. Colella, P., Sayana, R., Suarez-Nieto, M.V., Sarno, J., Nyame, K., Xiong Jian and Pimentel Vera, L.N., Arozqueta Basurto Jessica and Corbo, M., Limaye, A., Davis, K.L., Abu-Remaileh, M., et al. (2024). CNS-wide repopulation by hematopoietic-derived microglia-like cells corrects progranulin deficiency in mice. Nat Commun. Jul 5;15(1):5654.
74. Weinstock, N.I., Shin, D., Dhimal, N., Hong, X., Irons, E.E., Silvestri, N.J., Reed, C.B., Nguyen, D., Sampson, O., Cheng, Y.C., et al. (2020). Macrophages Expressing GALC Improve Peripheral Krabbe Disease by a Mechanism Independent of Cross-Correction. Neuron. Jul 8;107(1):65-81.e9.
75. Weinstock, N.I., Kreher, C., Favret, J., Nguyen, D., Bongarzone, E.R., Wrabetz, L., Laura Feltri, M., and Shin, D. (2020). Brainstem development requires galactosylceramidase and is critical for pathogenesis in a model of Krabbe disease. Nat Commun. Oct 23;11(1):5356.
76. Brendel, C., Rio, P., and Verhoeyen, E. (2020). Humanized mice are precious tools for evaluation of hematopoietic gene therapies and preclinical modeling to move towards a clinical trial. Biochem Farmacol. Apr:174:113711.
77. Meneghini, V., Lattanzi, A., Tiradani, L., Bravo, G., Morena, F., Sanvito, F., Calabria, A., Bringas, J., Fisher-Perkins, J.M., Dufour, J.P., et al. (2016). Pervasive supply of therapeutic lysosomal enzymes in the CNS of normal and Krabbe-affected non-human primates by intracerebral lentiviral gene therapy . EMBO Mol Med. May 2;8(5):489-510.
78. Amendola, M., Venneri, M.A., Biffi, A., Vigna, E., and Naldini, L. (2005). Coordinate dual-gene transgenesis by lentiviral vectors carrying synthetic bidirectional promoters. Nat Biotechnol. Jan;23(1):108-16.
79. Vigna, E., Amendola, M., Benedicenti, F., Simmons, A.D., Follenzi, A., and Naldini, L. (2005). Efficient Tet-dependent expression of human factor IX in vivo by a new self-regulating lentiviral vector. Molecular Therapy. May;11(5):763-75.
80. Ornaghi, F., Sala, D., Tedeschi, F., Maffia, M.C., Bazzucchi, M., Morena, F., Valsecchi, M., Aureli, M., Martino, S., and Gritti, A. (2020). Novel bicistronic lentiviral vectors correct β-Hexosaminidase deficiency in neural and hematopoietic stem cells and progeny: implications for in vivo and ex vivo gene therapy of GM2 gangliosidosis. Neurobiol Dis. Feb:134:104667.
81. Gritti, A., Molin, M.D., Foroni, C., and Bonfanti, L. (2009). Effects of developmental age, brain region, and time in culture on long-term proliferation and multipotency of neural stem cell populations. Journal of Comparative Neurology. Nov 20;517(3):333-49.
82. Ricca, A., Cascino, F., and Gritti, A. (2022). Isolation and Culture of Neural Stem/Progenitor Cells from the Postnatal Periventricular Region. In Methods in Molecular Biology. 2022:2389:11-31.
83. Castagnola, V., Deleye, L., Podestà, A., Jaho, E., Loiacono, F., Debellis, D., Trevisani, M., Ciobanu, D.Z., Armirotti, A., Pisani, F., et al. (2023). Interactions of Graphene Oxide and Few-Layer Graphene with the Blood-Brain Barrier. Nano Lett. Apr 12;23(7):2981-2990.

84. Piras, F., Riba, M., Petrillo, C., Lazarevic, D., Cuccovillo, I., Bartolaccini, S., Stupka, E., Gentner, B., Cittaro, D., Naldini, L., et al. (2017). Lentiviral vectors escape innate sensing but trigger p53 in human hematopoietic stem and progenitor cells. EMBO Mol Med. Sep;9(9):1198-1211.
85. Mangiameli, E., Freschi, M., Luciani, M., and Gritti, A. (2022). Generation of neuronal/glial mixed cultures from human induced pluripotent stem cells (hiPSCs). In Methods in Cell Biology. 2022:171:229-245.
86. Martino, S., Tiribuzi, R., Tortori, A., Conti, D., Visigalli, I., Lattanzi, A., Biffi, A., Gritti, A., and Orlacchio, A. (2009). Specific determination of β-galactocerebrosidase activity via competitive inhibition of β-galactosidase. Clin Chem. Mar;55(3):541-8.
87. Sala, D., Ornaghi, F., Morena, F., Argentati, C., Valsecchi, M., Alberizzi, V., Di Guardo, R., Bolino, A., Aureli, M., Martino, S., et al. (2022). Therapeutic advantages of combined gene/cell therapy strategies in a murine model of GM2 gangliosidosis. Mol Ther Methods Clin Dev. Mar 16:25:170-189.
88. Voorink-Moret, M., Goorden, S.M.I., van Kuilenburg, A.B.P., Wijburg, F.A., Ghauharali-van der Vlugt, J.M.M., Beers-Stet, F.S., Zoetekouw, A., Kulik, W., Hollak, C.E.M., and Vaz, F.M. (2018). Rapid screening for lipid storage disorders using biochemical markers. Expert center data and review of the literature. Mol Genet Metab. Feb;123(2):76-84.
89. Groener, J.E.M., Poorthuis, B.J.H.M., Kuiper, S., Helmond, M.T.J., Hollak, C.E.M., and Aerts, J.M.F.G. (2007). HPLC for simultaneous quantification of total ceramide, glucosylceramide, and ceramide trihexoside concentrations in plasma. Clin Chem. Apr;53(4):742-7.
90. Sidhu, R., Mikulka, C.R., Fujiwara, H., Sands, M.S., Schaffer, J.E., Ory, D.S., and Jiang, X. (2018). A HILIC-MS/MS method for simultaneous quantification of the lysosomal disease markers galactosylsphingosine and glucosylsphingosine in mouse serum. Biomedical Chromatography. Jul;32(7):e4235.
91. Valeri, E., Unali, G., Piras, F., Abou-Alezz, M., Pais, G., Benedicenti, F., Lidonnici, M.R., Cuccovillo, I., Castiglioni, I., Arévalo, S., et al. (2024). Removal of innate immune barriers allows efficient transduction of quiescent human hematopoietic stem cells. Molecular Therapy. Jan 3;32(1):124-139.

List of Figure Captions

Figure 1. LV-transduced HSPCs overexpress and secrete the IDUAsp.mGALC.APO enzyme.
(A) Schematic of LVs encoding for m*Galc* and chimeric constructs (IDSsp.m*Galc*.APO and IDUAsp.m*Galc*.APO). *Galc* sequence fused with mCherry. IDSsp, sp sequence of iduronate-2-sulphatase enzyme; IDUAsp, sp sequence of alpha-L-iduronidase. L = linker, APO = Apolipoprotein E II receptor binding domain. **(B)** VCN in TWI HSPCs transduced with the different LVs (100 MOI) and untransduced (UT) TWI controls after 10 days (bulk of colony-forming cells, CFC) or 14 days (liquid cultures, LC) in culture. Data are expressed as the mean (SD) (n=6-9 experiments, 2-3 technical replicates/experiment); One-way ANOVA followed by Tukey's multiple comparison test. UT values (black lines) are below the background threshold. **(C)** GALC activity in LC cultures (pellet and sup) from LV-transduced, UT WT, and TWI HSPCs. Data are the mean (SD), n=6-9 experiments, 1-3 technical replicates/experiment; Kruskal-Wallis test followed by Dunn's multiple comparison test. **(D)** GALC activity normalized on the VCN in LC cultures from LV-transduced TWI HSPCs (pellet and sup). Data are expressed as FOLD vs. LV.m*Galc*-transduced TWI HSPCs (red dotted line). Data are expressed as the mean (SD), n=6-9 experiments, 1-3 technical replicates/experiment; Kruskal-Wallis followed by Dunn's multiple comparison test. In the pellet, the fold increase of IDUAsp.mGALC.APO to IDSsp.mGALC.APO is reported. **(E)** Representative WB showing: i) GALC precursor protein (anti-mCherry antibody) in the sup of UT TWI (negative control) and transduced-HSPC progeny (LC); ii) GALC precursor protein and cleaved form (anti-GALC antibody) in the pellet of UT TWI (negative control) and transduced-HSPC progeny (LC). **(F)** mCherry concentration (surrogate for GALC, measured by ELISA assay) in pellet and sup of transduced HSPC progeny (LC). Data are the mean (SD). Pellet: n=4 experiments with 3 biological replicates/exp for pellets, 2 technical replicates. Sup: n=2 experiments with 3 biological replicates/experiments, 2 technical replicates. One-way ANOVA followed by Tukey's multiple comparison test for pellet, Kruskal-Wallis followed by Dunn's multiple comparison test for sup. **(G)** mCherry concentration (surrogate for GALC, measured by ELISA assay) in the sup enriched with mGALC and IDUAsp.mGALC.APO enzyme. Data are the mean (SD) calculated as mCherry concentration (pg/ml) at 1, 3 ,6 and 24 hours of incubation divided by the mCherry concentration recorded immediately after plating (time 0). n=2 experiments, 2 technical replicates/experiment. **(H)** Percentage of transcytosis of mCherry (surrogate for GALC, measured by ELISA assay) calculated as the ratio of mCherry after 24 hours (pg/ml) in the basolateral medium divided by mCherry at time 0, across a monolayer of bEND.3 endothelial cells in a transwell plate. Data represent the mean (SD), n=5-6 experiments, 1-3 technical replicates/experiment. Unpaired Student's T test. **(I)** Representative WB showing the GALC precursor protein (anti-mCherry antibody; 110 kDa) in the basolateral compartment of the transwell. Negative control: basolateral medium of a transwell incubated with the sup of UT TWI HSPC progeny (LC).

Figure 2. Chimeric GALC enzyme secreted by HSPC progeny rescues GALC activity, enhances uptake in acceptor cells, and reduces intracellular GalCer storage in TWI neural cells.
(A) Schematic representation of the cross-correction experiment. GALC-deficient neuronal/glial cell cultures (acceptor XC cells) are exposed for 24-72 hours to the GALC-enriched sup collected from LV-transduced donor cells (HSPC progeny or $CD14^+$-derived macrophages). At the end of the experiment, acceptor XC cells were

collected for analysis. **(B)** GALC activity measured in acceptor TWI XC neural cells treated for 72 hours with the sup collected from LV.m*Galc*-, LV.IDSsp.m*Galc*.APO-, LV.IDUAsp.m*Galc*.APO-transduced HSPC progeny (donor cells). The enzymatic activity is the percentage of normal levels (measured in WT neural cells). Data are expressed as the mean (SD), n =5-6 experiments, 1-2 technical replicates/experiment. One-way ANOVA followed by Tukey's multiple comparison test. **(C)** Uptake of mCherry (a surrogate for GALC) by XC TWI neural cells exposed to the sup enriched with mGALC and IDUAsp.mGALC.APO. The ELISA assay measured mCherry concentration (pg/ml) in the cell lysate of acceptor cells. Data are expressed as the mean (SD), n=3 experiments, 2 technical replicates/experiment, and analysed by the Mann-Whitney test. **(D)** Representative confocal IF pictures and insets showing the reduction in GalCer storage (green) in TWI XC neural cells treated with the sup of donor cells compared to the UT TWI counterpart. Nuclei stained with Hoechst (grey, pseudocolour); n=2–4 experiments, 2 coverslips/group/experiment. 63X magnification. Scale bar: 30 µm.

Figure 3. HSPC-GT in neonatal TWI mice using a chimeric enzyme.

(A) Experimental plan. Neonatal (PND 1-2) TWI and WT mice are myeloablated by a single intraperitoneal injection of BUS (20 mg/Kg). Transplantation of LV-transduced WT HSPCs expressing GFP (HSPC-T GFP WT) or LV-transduced TWI HSPCs expressing mGALC (HSPC-GT mGALC TWI) or IDUAsp.mGALC.APO (HSPC-GT IDUAsp.mGALC.APO TWI) is performed the following day. Treated TWI mice and age-matched UT WT and UT TWI controls are analysed one month after transplant and at the end of the experiment (human disease endpoint; > 39 days, the average lifespan of UT TWI mice). **(B)** Percentage of donor-derived $CD45^+$ cells (GFP^+ WT HSPCs; $mCherry^+$ TWI HSPCs) measured in the PB of treated TWI mice one month after transplant. Data are expressed as the mean. Each dot represents one mouse. **(C)** Body weight of treated TWI mice (GFP WT: n=11; mGALC: n=6; IDUAsp.mGALC.APO: n=8), UT WT (n=10), and UT TWI (n=14), registered starting at 20 days of age. **(D)** Kaplan-Meier survival curves showing the survival percentage of treated and UT TWI mice. UT TWI: n=40; GFP WT: n=11; mGALC: n=6; IDUAsp.mGALC.APO: n=8. Data analysed using the Log Rank (Mantel-Cox) test. **(E)** Enzymatic GALC activity measured in CNS tissues (brain and spinal cord), PNS tissue (sciatic nerve), peripheral organs (liver, spleen), and BM of treated mice and UT controls (WT and TWI) at the end of the experiment. Data are expressed as the mean (SD). n=2-3 experiments, each dot represents one mouse. Kruskal-Wallis test followed by Dunn's multiple comparison test vs UT WT.

Figure 4. Engraftment of HSPC myeloid progeny in the brain of HSPC-GT-treated TWI mice and *in vivo* cross-correction.

(A) Representative fluorescence pictures of sagittal brain slices showing the distribution of engrafted $mCherry^+$ cells (red) in the brain of HSPC-GT IDUAsp.mGALC.APO TWI analysed at PND 43. Nuclei stained with Hoechst (grey, pseudocolour). 20X magnification. Scale bars 1000 µm, n = 3 sagittal sections. **(B)** Representative fluorescence pictures show the chimeric GALC enzyme's expression (mCherry+ signal, red) in LV.IDUAsp.m*Galc*.APO HSPC-derived myeloid progeny ($CD68^+$ cells, blue) and its uptake by GALC-deficient astrocytes ($GFAP^+$ cells, green). Hippocampal region, 40X magnification. Scale bar 30 µm, n = 3 sagittal sections. **(B')** Magnification of the picture in B. Scale bar 10 µm. **(C)** Representative fluorescence pictures show the chimer

GALC enzyme's expression (mCherry+ signal, red) in LV.IDUAsp.m*Galc*.APO HSPC-derived myeloid progeny (CD68$^+$ cells, blue) and its uptake by GALC-deficient neurons (NeuN$^+$ cells, green). Hippocampal region, 40X magnification. Scale bar 30 μm, n = 3 sagittal sections. **(C')** Magnification of the picture in C. Scale bar 10 μm. **(D)** Representative fluorescence picture showing the correct lysosomal (LAMP1$^+$ signal, blue) of chimeric IDUAsp.mGALC.APO enzyme (mCherry+ signal, red) in the GALC-deficient neurons (NeuN$^+$ cells, green). Cortical region, 40X magnification. Scale bar 30 μm, n = 3 sagittal sections. **(D')** Magnification of the picture in D. Scale bar 5 μm.

Figure 5. Robust and safe LV-mediated gene transfer in human CD34$^+$ HSPC and CD14$^+$ progeny and efficient cross-correction of human GLD neural cells.

(A) Schematic of LV encoding for h*GALC* and h*GALC* chimeric constructs (LV.IDSsp.h*GALC*.APO and LV.IDUAsp.h*GALC*.APO). The miRNA tag 126 (mirT126) was included in the original codon-optimized h*GALC* sequence.[44] **(B)** VCN in CD34$^+$ HSPCs transduced with LV.h*GALC*, LV.IDSsp.h*GALC*.APO, LV.IDUAsp.h*GALC*.APO, LV.GFP (100 MOI) and UT HD control after 10 days (bulk of colony-forming cells, CFC) or 14 days (liquid cultures, LC) in culture. Data are expressed as the mean (SD), n=5-6 independent experiments, 2 technical replicates/experiment. UT values (black lines) are below the background threshold. **(C)** GALC activity measured in pellets of UT and LV-transduced HSPC progeny (LC). Data are expressed as the mean (SD), n=5-6 experiments, 2 technical replicates/experiments. One-way ANOVA followed by Tukey's multiple comparison test; GALC activity (normalized on the VCN) measured in pellets of UT and LV-transduced HSPC progeny (LC). Data are expressed as the mean (SD), n=5-6 experiments, 2 technical replicates/experiment. One-way ANOVA followed by Tukey's multiple comparison test. The fold increase of IDUAsp.hGALC.APO to IDSsp.hGALC.APO is reported. **(D-E)** Representative WB (D) and quantification (E) showing GALC precursor protein (80 kDa) and processed forms (50 kDa and 30 kDa) in pellet and sup of UT and LV-transduced CD34$^+$ HSPC progeny (LC). Actin was used as a normalizer in pellets. Data in E are expressed as GALC/ACTIN/VCN in pellets and GALC/VCN in sup, mean (SD), n=3 experiments, 1 technical replicate/experiment. Unpaired Student's t-test. **(F)** VCN measured 9 days post-transduction in HD and GLD CD14$^+$-derived macrophages; n=6 HD, n=2 GLD. Data are expressed as the mean, n=3 experiments, 1-2 technical replicates/experiment. Each shape represents 1 donor *(legend in G).* **(G)** GALC activity in UT and LV-transduced CD14$^+$-derived macrophages (pellets and sup). n= 6 HD, n=2 GLD. Data are expressed as the mean, n=3 experiments, 1-2 technical replicates/experiment. Each shape represents 1 donor. **(H)** GALC activity in XC GLD hiPSC-derived neural acceptor cells treated for 24 hours with the sup from UT and LV-transduced HD and GLD CD14$^+$-derived macrophages (donor cells). The enzymatic activity is expressed as a percentage of the normal level (measured in HD hiPSC-derived neural cells). n=2 experiments, 1-2 technical replicates. **(I)** GALC activity in XC GLD hiPSC-derived neural acceptor cells treated for 24 hours with the sup from UT and LV-transduced HD CD34$^+$ HSPC progeny (donor cells). The enzymatic activity is expressed as a percentage of the normal level (measured in HD hiPSC-derived neural cells). Mean (SD), n=3-6 experiment, 1-2 technical replicates/experiment. **(J)** Psychosine content in XC GLD iPSC-derived neural acceptor cells exposed for 24 hours to the sup of LV-transduced HD CD34$^+$ HSPC progeny (donor cells). Data are expressed as the mean (SD), n=3 experiments, 1-2 replicates/experiment. One-way ANOVA followed by Tukey's multiple comparison test.

Figure 6. Persistent gene transfer and enhanced bioavailability upon xenotransplantation of LV-transduced CD34$^+$ HSPCs in NSG mice.

(A) Engraftment levels (percentage of hCD45$^+$ cells) in the PB of NSG mice at 4, 8 and 12 weeks post-transplantation. Data are expressed as the mean, n=3 experiments, each dot represents one mouse *(legend in C)*. **(B)** GALC activity in the sera of transplanted NSG mice at 8 weeks post-transplant. Data are expressed as the mean. One-way ANOVA, followed by Tukey's multiple comparison test. n=1 experiment, each dot represents one mouse *(legend in C)*. **(C)** GALC activity in the sera normalized on the percentage of engraftment in PB at 8 weeks. Data are expressed as the mean. One-way ANOVA, followed by Tukey's multiple comparison test. n=1 experiment, each dot represents one mouse. Fold change: IDUAsp.hGALC.APO vs hGALC, 2X; IDUAsp.hGALC.APO vs GFP, 2.3X; GALC vs GFP, 1.2X. **(D)** VCN measured in the BM of transplanted NSG mice at the time of sacrifice (16 weeks). Data are expressed as the mean. n=2 experiment, each dot represents one mouse *(legend in E)*. **(E)** Percentage of hCD45$^+$ (left) and hCD34$^+$ cells (right) in the BM of transplanted NSG mice. Data are expressed as the mean. n=1 experiment, each dot represents one mouse. **(F)** Cell composition (expressed in percentage of total cells) in the BM of transplanted NSG mice at the time of sacrifice (16 weeks); GFP: n=3 mice, hGALC: n=6 mice, IDUAsp.hGALC.APO: n=6 mice). Progenitors (CD34$^+$CD38$^{+/-}$, left), myeloid cells and B lymphocytes (CD33$^+$ and CD19$^+$, respectively, right) are represented in different colours. Data are expressed as the mean (SD), n=1 experiment. **(G)** Analyses on the spleen of transplanted NSG mice at 16 weeks: GALC activity (left), data are expressed as the mean and analysed by Kruskal-Wallis test followed by Dunn's multiple comparison test; percentage of hCD45$^+$ cells (middle) and GALC activity normalized on the percentage of engrafted hCD45$^+$ cells (right), data are expressed as the mean and analysed by One-way ANOVA followed by Tukey's multiple comparison test. n=1 experiment, each dot represents one mouse *(legend in H)*. **(H)** GALC activity in the spleen normalized on the percentage of engraftment in the PB at 12 weeks. Data are expressed as the mean. One-way ANOVA followed by Tukey's multiple comparison test. n=1 experiment, each dot represents one mouse. **(I)** Analyses on the liver of transplanted NSG mice at 16 weeks: absolute GALC activity (left) and normalized on the percentage of engraftment in the PB at 12 weeks (right). Data are expressed as the mean and analysed by One-way ANOVA followed by Tukey's multiple comparison test. n=1 experiment, each dot represents one mouse. **(J)** Analyses on the brain of transplanted NSG mice at 16 weeks: absolute GALC activity (left) and normalized on the percentage of engraftment in the PB at 12 weeks (right). Data are expressed as the mean and analysed using the Unpaired Student's t-test. n=2 experiments, each dot represents one mouse.

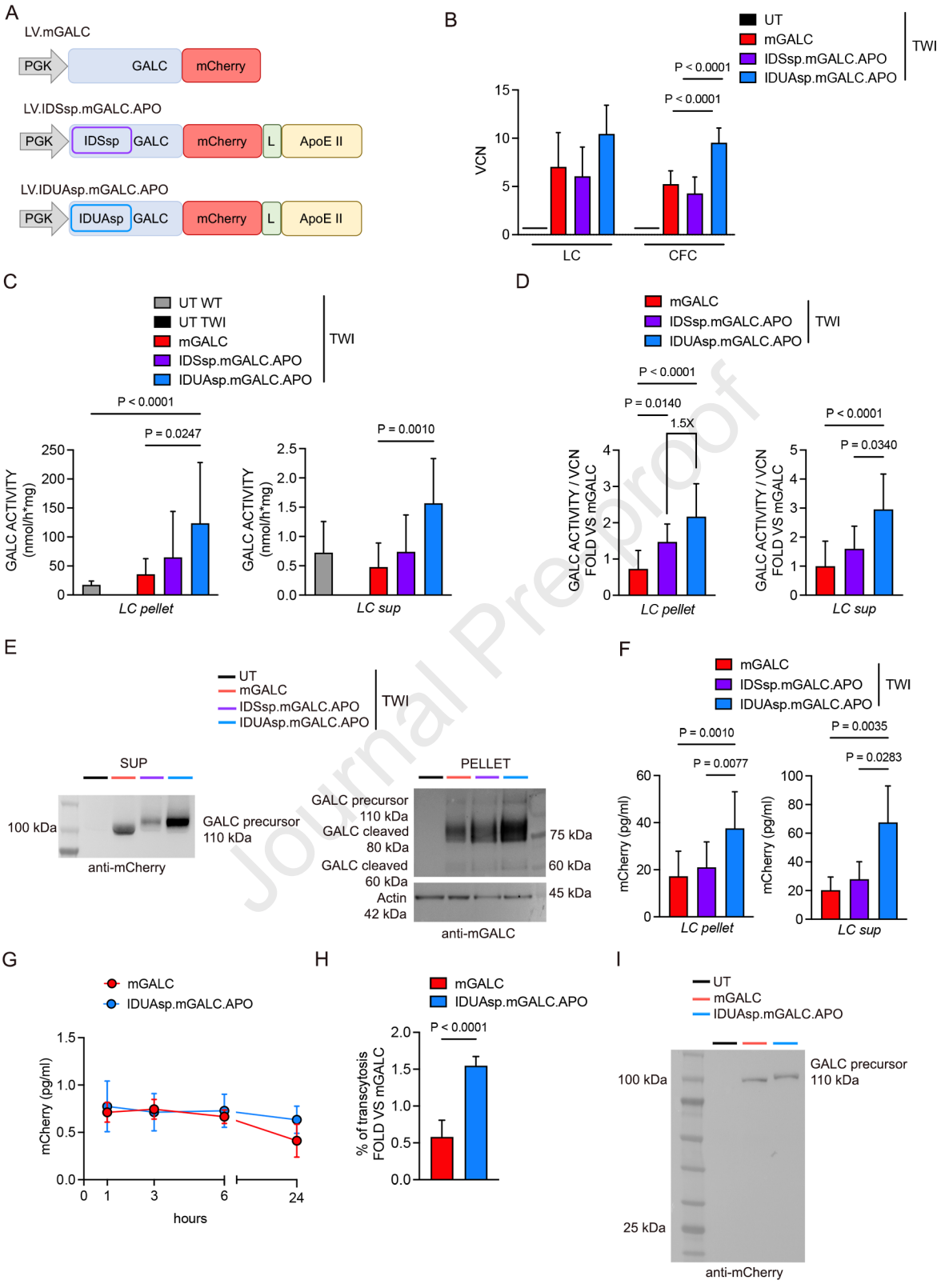

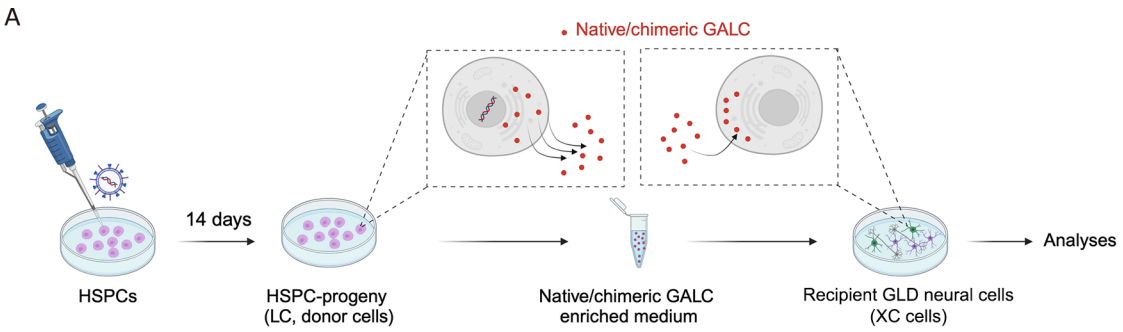

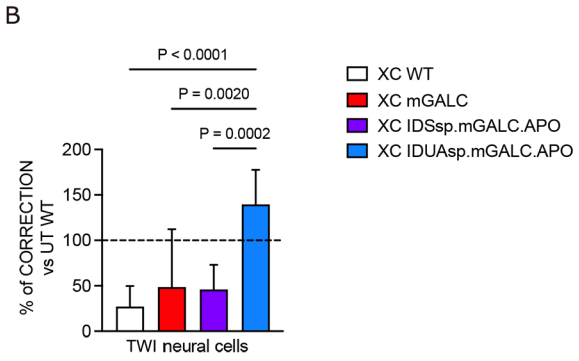

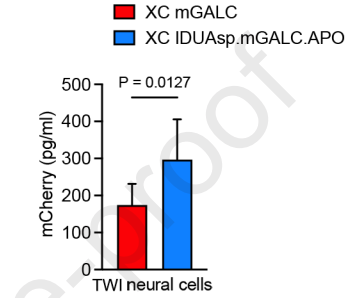

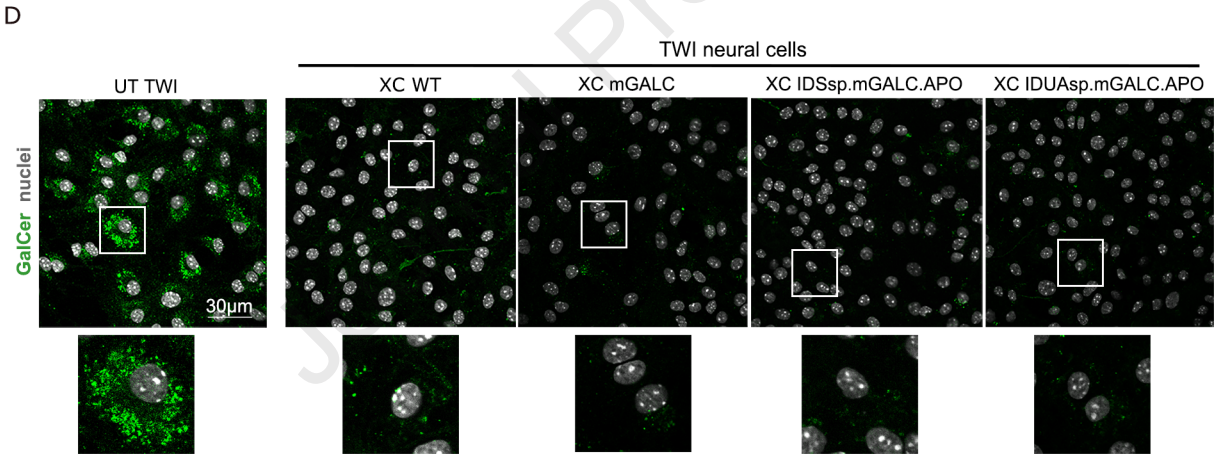

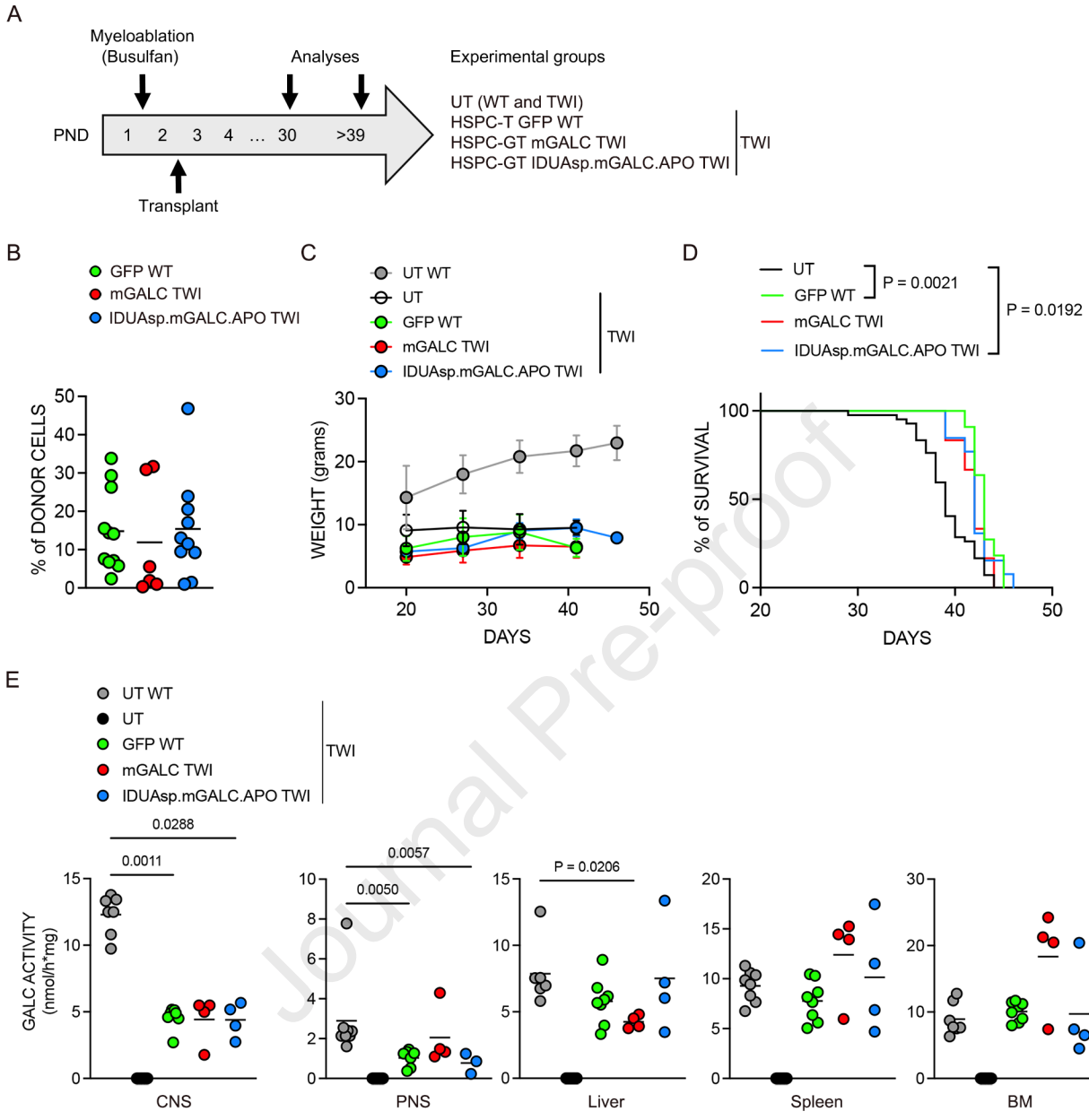

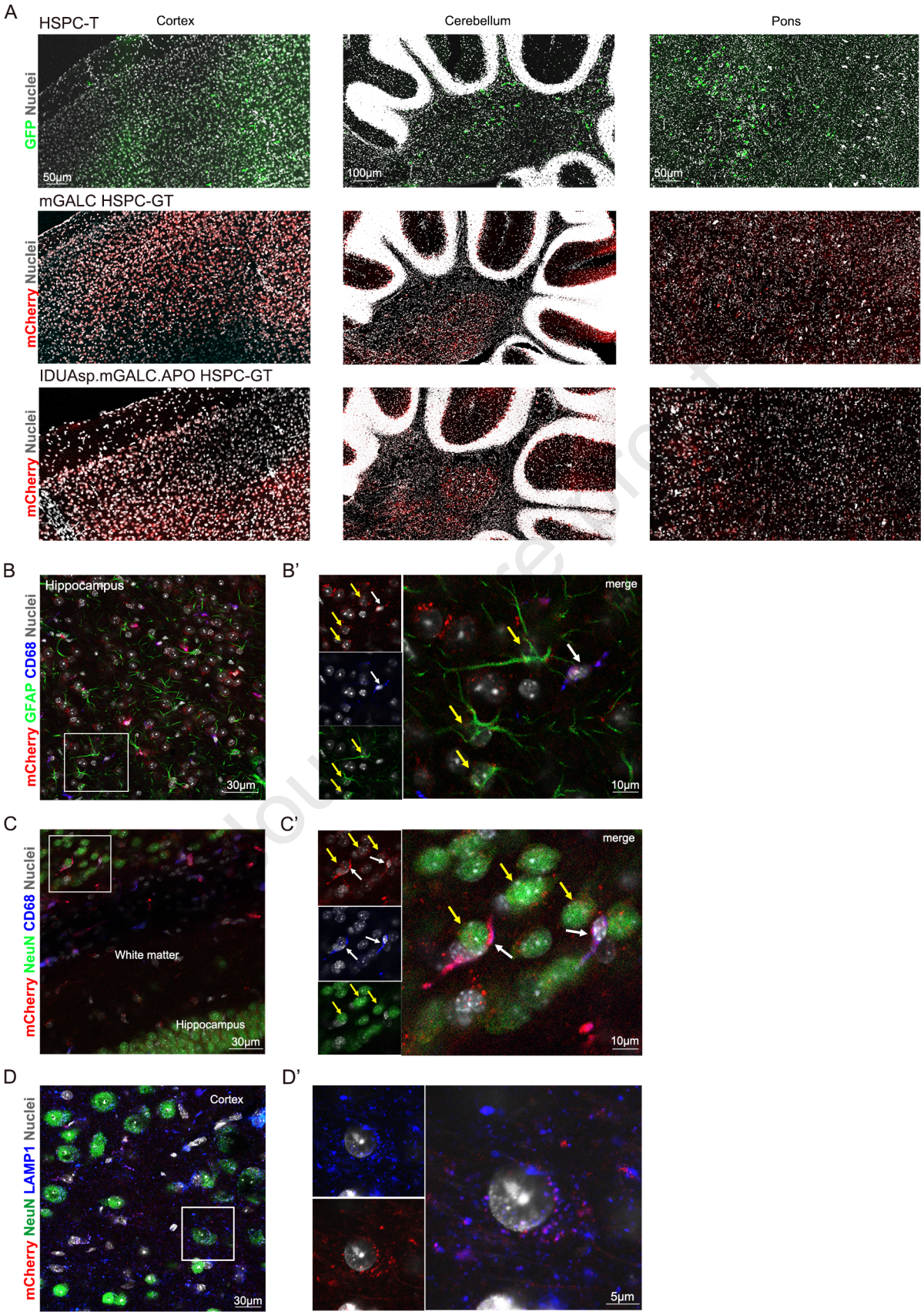
A
HSPC-T
Cortex
Cerebellum
Pons
GFP Nuclei
50µm
100µm
50µm
mGALC HSPC-GT
mCherry Nuclei
IDUAsp.mGALC.APO HSPC-GT
mCherry Nuclei
B
Hippocampus
mCherry GFAP CD68 Nuclei
30µm
B'
merge
10µm
C
White matter
Hippocampus
mCherry NeuN CD68 Nuclei
30µm
C'
merge
10µm
D
Cortex
mCherry NeuN LAMP1 Nuclei
30µm
D'
5µm

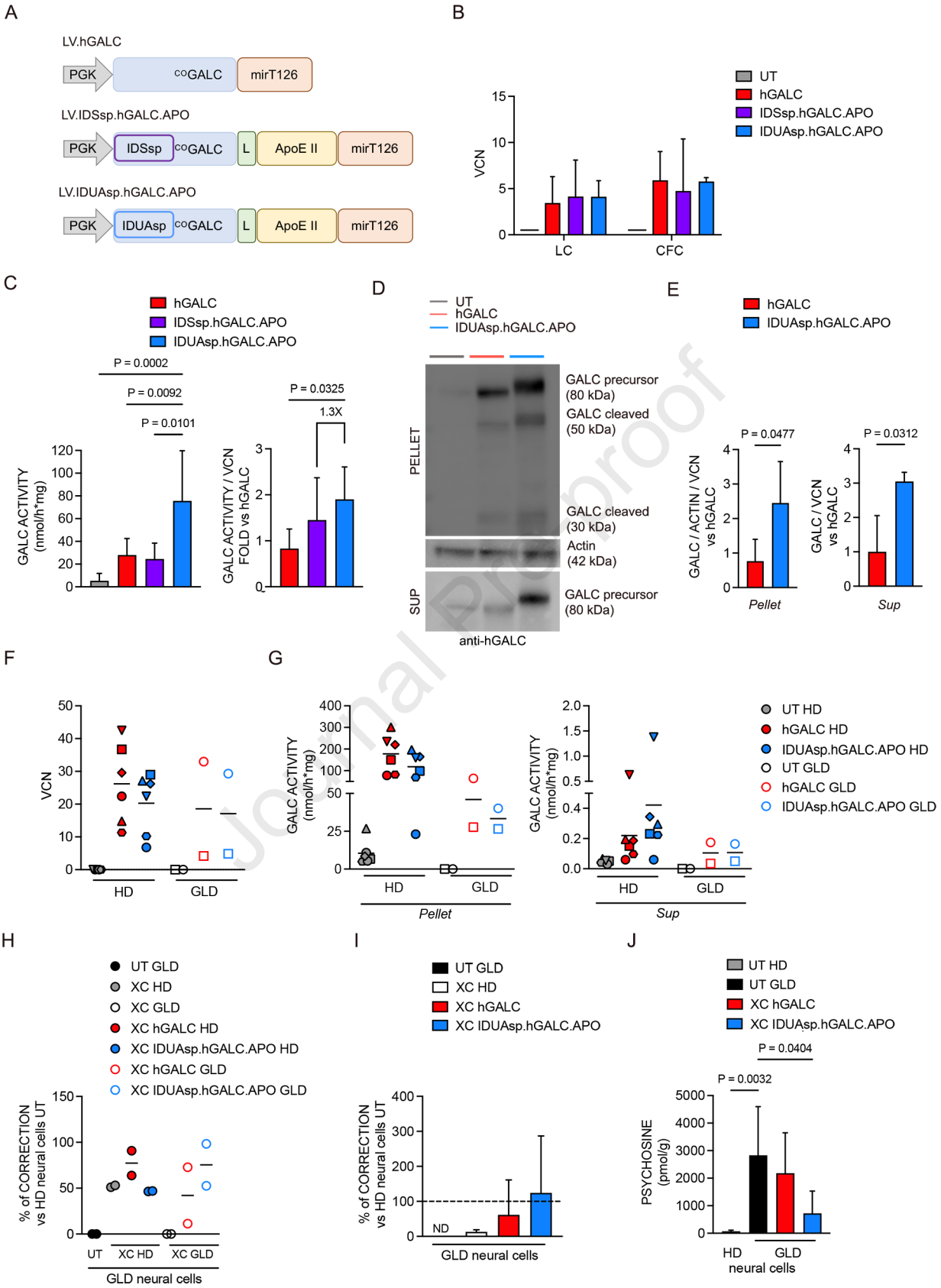

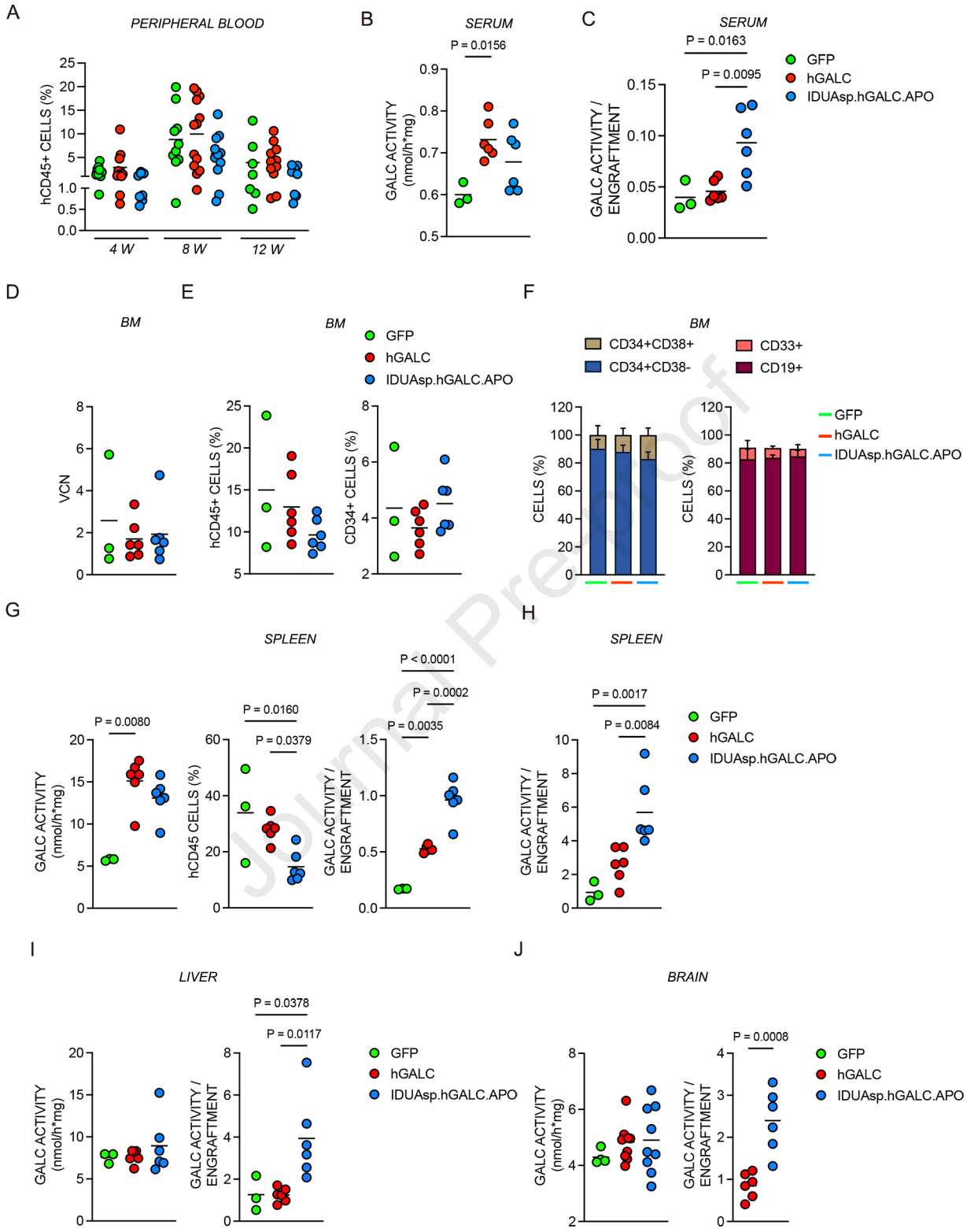
A
PERIPHERAL BLOOD
hCD45+ CELLS (%)
4 W
8 W
12 W
B
SERUM
P = 0.0156
GALC ACTIVITY (nmol/h*mg)
C
SERUM
P = 0.0163
P = 0.0095
GALC ACTIVITY / ENGRAFTMENT
GFP
hGALC
IDUAsp.hGALC.APO
D
BM
VCN
E
BM
hCD45+ CELLS (%)
CD34+ CELLS (%)
F
BM
CD34+CD38+
CD34+CD38-
CD33+
CD19+
CELLS (%)
G
SPLEEN
P = 0.0080
GALC ACTIVITY (nmol/h*mg)
P = 0.0160
P = 0.0379
hCD45 CELLS (%)
P < 0.0001
P = 0.0002
P = 0.0035
GALC ACTIVITY / ENGRAFTMENT
H
SPLEEN
P = 0.0017
P = 0.0084
GALC ACTIVITY / ENGRAFTMENT
I
LIVER
P = 0.0378
P = 0.0117
GALC ACTIVITY (nmol/h*mg)
GALC ACTIVITY / ENGRAFTMENT
J
BRAIN
P = 0.0008
GALC ACTIVITY (nmol/h*mg)
GALC ACTIVITY / ENGRAFTMENT

Gritti and colleagues developed a lentiviral vector expressing a chimeric GALC enzyme with enhanced production, secretion, and cross-correction. Their studies in murine models and patient-derived cells showed stable gene marking, increased bioavailability, and effective CNS and PNS delivery, demonstrating the therapeutic potential of chimeric GALC in HSPC GT for GLD.